


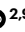






Intrathecal bivalent CAR T cells targeting EGFR and IL13R α 2 in recurrent glioblastoma: phase 1 trial interim results

Received: 16 February 2024

Accepted: 29 February 2024

Published online: 13 March 2024

 Check for updates

Stephen J. Bagley ^{1,2,12}✉, Meghan Logun ^{2,3,12}, Joseph A. Fraietta^{4,5}, Xin Wang⁶, Arati S. Desai^{1,2}, Linda J. Bagley^{3,7}, Ali Nabavizadeh⁷, Danuta Jarocha⁴, Rene Martins⁴, Eileen Maloney^{2,3}, Lester Lledo⁴, Carly Stein⁴, Amy Marshall⁴, Rachel Leskowitz⁴, Julie K. Jadowsky ⁴, Shannon Christensen⁴, Bike Su Oner⁴, Gabriela Plesa⁴, Andrea Brennan⁴, Vanessa Gonzalez⁴, Fang Chen ⁴, Yusha Sun^{2,6}, Whitney Gladney⁸, David Barrett⁸, MacLean P. Nasrallah ^{2,9}, Wei-Ting Hwang ¹⁰, Guo-Li Ming ^{6,11}, Hongjun Song ^{2,6,11}, Donald L. Siegel ^{2,4,9}, Carl H. June ^{4,9}, Elizabeth O. Hexner ^{1,4}, Zev A. Binder^{2,3,4,12} & Donald M. O'Rourke ^{2,3,4,12}✉

Recurrent glioblastoma (rGBM) remains a major unmet medical need, with a median overall survival of less than 1 year. Here we report the first six patients with rGBM treated in a phase 1 trial of intrathecally delivered bivalent chimeric antigen receptor (CAR) T cells targeting epidermal growth factor receptor (EGFR) and interleukin-13 receptor alpha 2 (IL13R α 2). The study's primary endpoints were safety and determination of the maximum tolerated dose. Secondary endpoints reported in this interim analysis include the frequency of manufacturing failures and objective radiographic response (ORR) according to modified Response Assessment in Neuro-Oncology criteria. All six patients had progressive, multifocal disease at the time of treatment. In both dose level 1 (1×10^7 cells; $n = 3$) and dose level 2 (2.5×10^7 cells; $n = 3$), administration of CART-EGFR-IL13R α 2 cells was associated with early-onset neurotoxicity, most consistent with immune effector cell-associated neurotoxicity syndrome (ICANS), and managed with high-dose dexamethasone and anakinra (anti-IL1R). One patient in dose level 2 experienced a dose-limiting toxicity (grade 3 anorexia, generalized muscle weakness and fatigue). Reductions in enhancement and tumor size at early magnetic resonance imaging timepoints were observed in all six patients; however, none met criteria for ORR. In exploratory endpoint analyses, substantial CAR T cell abundance and cytokine release in the cerebrospinal fluid were detected in all six patients. Taken together, these first-in-human data demonstrate the preliminary safety and bioactivity of CART-EGFR-IL13R α 2 cells in rGBM. An encouraging early efficacy signal was also detected and requires confirmation with additional patients and longer follow-up time. ClinicalTrials.gov identifier: [NCT05168423](https://clinicaltrials.gov/ct2/show/study/NCT05168423).

A full list of affiliations appears at the end of the paper. ✉ e-mail: sbagley@penmedicine.upenn.edu; donald.orourke@penmedicine.upenn.edu

Table 1 | Baseline patient characteristics

Patient	Sex	Age	Race	Ethnicity	EGFR alteration(s) detected in tumor immediately before CAR T cell treatment	MGMT promoter methylation	No. of relapses at time of CAR T cell treatment	Previous treatment	No. of months from last RT	KPS on day 0
1	Male	71	Caucasian	Non-Hispanic	EGFR amplification, EGFR R108K	Unmethylated	2nd relapse	RT (60 Gy), TMZ, TTFields	9	80
2	Male	50	Unknown	Non-Hispanic	EGFR amplification, EGFRvIII	Unmethylated	2nd relapse	RT (60 Gy), TMZ, osimertinib	11	80
3	Male	66	Caucasian	Non-Hispanic	EGFR amplification, EGFRvIII	Methylated	2nd relapse	RT (60 Gy), TMZ, lomustine, bevacizumab	21	60
4	Male	66	Caucasian	Non-Hispanic	EGFR amplification	Unmethylated	1st relapse	RT (60 Gy), TMZ	20	90
5	Male	65	Caucasian	Non-Hispanic	EGFR amplification	Unmethylated	1st relapse	RT (60 Gy), TMZ	6	80
6	Male	33	Caucasian	Non-Hispanic	EGFR amplification	Methylated	3rd relapse	RT × 2 (60 Gy, 35 Gy), TMZ, lomustine	23	70

MGMT, O6-methylguanine-DNA methyltransferase; RT, radiotherapy; TMZ, temozolomide; TTFields, tumor-treating fields.

Glioblastoma (GBM) is the most common and lethal primary brain cancer in adults. There is currently no standard treatment for relapsed disease after first-line chemoradiotherapy, and median overall survival (OS) for recurrent GBM (rGBM) is less than 1 year¹. Effective therapy for rGBM remains one of the greatest unmet medical needs in oncology.

Chimeric antigen receptor (CAR) T cells targeting the GBM-specific and associated antigens epidermal growth factor receptor deletion mutant variant III (EGFRvIII)^{2,3}, human epidermal growth factor receptor 2 (HER2)⁴, interleukin-13 receptor alpha 2 (IL13Rα2)^{5,6}, erythropoietin-producing human hepatocellular carcinoma A2 (EphA2)⁷ and the GD2 disialoganglioside⁸ were previously evaluated in phase 1 studies using both intravenous and intrathecal delivery methods. These approaches have demonstrated acceptable toxicity profiles but have shown limited evidence of efficacy in adults with GBM aside from isolated case reports^{6,9}. Resistance mechanisms identified through translational studies include a highly immunosuppressive tumor microenvironment, intrinsic T cell dysfunction and tumor antigen heterogeneity leading to antigen escape^{2,10–12}.

To address the problem of tumor heterogeneity in the setting of monovalent chimeric antigen receptor (CAR) T cell therapy and improve the efficacy of CAR T cells for GBM, we developed a bivalent CAR T cell product to simultaneously target EGFR and IL13Rα2 (Extended Data Fig. 1a)¹³. Autologous T cells are transduced with a bicistronic lentiviral vector containing both a chimeric scFv targeting the EGFR epitope 806 (ref. 14), a cryptic, conformational epitope that is predominantly accessible when dysregulation of EGFR activation occurs due to overexpression (EGFR amplification) and/or the presence of EGFR extracellular domain mutations^{15–17}, as well as a humanized scFv targeting the tumor-associated antigen IL13Rα2 (ref. 18). EGFR epitope 806 is expected to be present on the tumor surface in 50–60% of patients with GBM¹⁹, and the 806 scFv used in our product has previously demonstrated a lack of binding against physiologic EGFR found on astrocytes and keratinocytes, establishing its tumor specificity and abrogating concerns for on-target/off-tumor toxicity¹⁴. IL13Rα2 is expressed in 50–75% of patients with GBM^{5,20} and has previously demonstrated promise as a target for cellular therapy in this disease⁶.

We initiated a first-in-human clinical trial to evaluate the feasibility, safety, bioactivity and therapeutic potential of CART-EGFR-IL13Rα2 cells for patients with rGBM (ClinicalTrials.gov identifier: [NCT05168423](https://clinicaltrials.gov/ct2/show/study/NCT05168423)). Here we report a non-prespecified interim analysis of the patients treated at the first two dose levels: 1×10^7 CART-EGFR-IL13Rα2 cells ($n = 3$) and 2.5×10^7 CART-EGFR-IL13Rα2 cells ($n = 3$) (CONSORT diagram; Extended Data Fig. 1b). The data cutoff for this report was 2 February 2024 with a median follow-up time of 2.5 months (range,

1–7.5 months) for the six patients treated. The first patient was treated on 14 June 2023, and the sixth patient was treated on 4 January 2024.

Results

Study design and patients

This is an ongoing single-center, phase 1, open-label study of adult patients 18 years of age or older with rGBM. Full study eligibility criteria are provided in the Study Protocol. Key inclusion criteria include isocitrate dehydrogenase (IDH) wild-type GBM that has recurred after prior radiotherapy and presence of EGFR amplification by fluorescence in situ hybridization (FISH) on any prior tumor tissue specimen. Presence of IL13Rα2 is not required as a study inclusion criterion due to the current lack of a validated assay for detecting and/or quantifying its expression. Key exclusion criteria include receipt of bevacizumab within 3 months before registration and tumors localized primarily to the brainstem or spinal cord. Using a 3 + 3 dose-escalation design, three dose levels (1×10^7 , 2.5×10^7 and 5×10^7 cells) of CART-EGFR-IL13Rα2 cells are being explored. The cell product is injected intrathecally as a single dose through an intraventricular reservoir. The observation period for dose-limiting toxicity (DLT) is 28 d. The primary objective of the study is to evaluate the safety of CART-EGFR-IL13Rα2 cells in patients with rGBM. Secondary objectives are to evaluate manufacturing feasibility and to describe preliminary efficacy. Primary endpoints include occurrence of DLT, determination of the maximum tolerated dose and the type, frequency, severity and attribution of adverse events (AEs) and serious adverse events (SAEs). Secondary endpoints include the proportion of patients enrolled on this study who receive study treatment, frequency of manufacturing failures (ability to meet targeted dose and cell product volume restrictions), progression-free survival (PFS), objective response rate (ORR), duration of response (DOR) and OS. Up to 18 patients may be treated. The protocol was approved by the institutional review board of the University of Pennsylvania (protocol 850297). Patients provided written informed consent. Patient baseline characteristics are displayed in Table 1, and product information for each patient is provided in Extended Data Table 1. IL13Rα2 CAR expression values, although not used as part of the product release criteria, were low relative to EGFR expression. We have since modified our approach, and updated CAR expression values are presented in Supplementary Table 1 with corresponding flow cytometry plots in Extended Data Fig. 2.

Treatment and study assessments

Potential candidates for this study may undergo leukapheresis at any time starting 1 month after completion of first-line radiotherapy (Extended Data Fig. 1c). At the time of suspected recurrence/

Table 2 | All cohort 1 AEs that occurred after T cell administration and up to day 28

Category	Grades					Total
	1	2	3	4	5	
Blood and lymphatic system disorders	1	0	0	0	0	1
Anemia	1	0	0	0	0	1
Cardiac disorders	1	0	0	0	0	1
Sinus bradycardia	1	0	0	0	0	1
Gastrointestinal disorders	3	2	0	0	0	5
Constipation	2	1	0	0	0	3
Nausea	1	0	0	0	0	1
Vomiting	0	1	0	0	0	1
General disorders and administration site conditions	1	0	0	0	0	1
Edema limbs	1	0	0	0	0	1
Immune system disorders	3	0	0	0	0	3
CRS	3	0	0	0	0	3
Investigations	6	1	2	0	0	9
ALT increased	1	0	0	0	0	1
Fibrinogen decreased	2	0	0	0	0	2
Fibrinogen decreased.	1	0	0	0	0	1
Lipase increased	1	1	0	0	0	2
Lymphocyte count decreased	0	0	2	0	0	2
Serum amylase increased	1	0	0	0	0	1
Metabolism and nutrition disorders	1	1	0	0	0	2
Hypokalemia	1	0	0	0	0	1
Hyponatremia	0	1	0	0	0	1
Musculoskeletal and connective tissue disorders	2	0	0	0	0	2
Flank pain	1	0	0	0	0	1
Generalized muscle weakness	1	0	0	0	0	1
Nervous system disorders	1	2	2	0	0	5
Facial muscle weakness	1	0	0	0	0	1
Headache	0	1	0	0	0	1
Nervous system disorders—other (CAR neurotoxicity)	0	1	2	0	0	3
Psychiatric disorders	1	1	0	0	0	2
Delirium	0	1	0	0	0	1
Insomnia	1	0	0	0	0	1
Renal and urinary disorders	0	2	0	0	0	2
Urinary incontinence	0	1	0	0	0	1
Urinary retention	0	1	0	0	0	1
Respiratory, thoracic and mediastinal disorders	1	1	0	0	0	2
Hiccups	1	0	0	0	0	1
Hypoxia	0	1	0	0	0	1
Skin and subcutaneous tissue disorders	0	0	1	0	0	1
Skin ulceration ^a	0	0	1	0	0	1
Vascular disorders	1	1	0	0	0	2
Flushing	1	0	0	0	0	1
Hypotension	0	1	0	0	0	1
Total	22	11	5	0	0	38

^aGrade 3 skin ulceration in one patient was a sacral pressure ulcer.

progression, consent is obtained to enroll in the treatment phase. During cell product manufacturing, surgery is performed for (1) maximal safe resection of tumor and confirmation that the target (as assessed by presence of EGFR amplification) has remained present at relapse and (2) placement of an intraventricular subcutaneous reservoir (Ommaya). As soon as possible upon recovery from surgery, patients are admitted to the hospital for a single intrathecal dose of CART-EGFR-IL13R α 2 cells. The first three patients described in this report were treated at dose level 1 (1×10^7 cells), and the second three patients were treated at dose level 2 (2.5×10^7 cells). Patients were monitored in the hospital for a minimum of 7 d. Cytokine release syndrome (CRS) was graded according to American Society for Transplantation and Cellular Therapy (ASTCT) criteria (Supplementary Table 2), and neurotoxicity was graded using a modified immune effector-associated neurotoxicity syndrome (ICANS) severity system that integrated baseline neurologic deficits in this population (Supplementary Table 3). Magnetic resonance imaging (MRI) of the brain with and without gadolinium was scheduled per protocol 24–48 h after CART cell administration, on day 28 and monthly thereafter (± 7 d). Modified Response Assessment in Neuro-Oncology (mRANO) criteria²¹ were used to assess response.

Safety and AEs

A complete list of AEs is provided in Table 2 (dose level 1) and Table 3 (dose level 2). Duration between date of surgery and receipt of CAR T cells ranged from 17 d to 35 d and is provided for each patient in Extended Data Table 1. All six patients experienced early and moderate-severe neurotoxicity with elements of both ICANS and tumor inflammation-associated neurotoxicity (TIAN)²², with no appreciable differences in the type or grade of neurotoxicity in patients treated at dose level 1 (patients 1, 2 and 3) versus dose level 2 (patients 4, 5 and 6). No patients demonstrated radiographic evidence of elevated intracranial pressure or clinical signs of herniation or required acute neurosurgical intervention. CAR neurotoxicity was accompanied by low-grade cytokine release syndrome (CRS) in all six patients. At dose level 1, CRS was grade 1 (fevers only) in all patients. At dose level 2, both grade 1 ($n = 1$) and grade 2 ($n = 2$) CRS was observed. One patient (patient 5) treated at dose level 2 experienced events that met the definition of a DLT. One patient (patient 3) required monitoring temporarily in the medical intensive care unit, whereas all other patients were cared for entirely on routine medical floors. Intracranial pressure monitoring was not performed in any patient. The clinical courses and management of CAR neurotoxicity, graded according to Supplementary Table 3, are described for each patient in the subsequent sections.

Patient 1 developed grade 2 CAR neurotoxicity approximately 10 h after CAR T cell administration (day 0), characterized by increasing confusion, acute worsening of chronic aphasia and nausea and vomiting. Dexamethasone and anakinra (IL-1R antagonist) were initiated with improvement in the patient's neurologic status by day +2. Patient 2, who was noted on the day -1 MRI to have rapid tumor progression, developed acute worsening of chronic left facial weakness and aphasia on day +1, consistent with grade 3 CAR neurotoxicity and prompting treatment with dexamethasone and anakinra. Improvement in neurologic symptoms back to baseline was noted by day +2. In patient 3, who entered the study with worsening leptomeningeal disease and declining performance status, a reduction in the immune effector cell encephalopathy (ICE) score was noted on day +1. The patient was diagnosed with grade 3 CAR neurotoxicity and treated with dexamethasone and anakinra. The patient's level of alertness and orientation waxed and waned over the subsequent 24 h, ultimately culminating in the patient becoming difficult to arouse verbally and being transferred to intensive care. Intubation was not required. Improvement in mental status was noted on day +4 with continued supportive care, and the patient returned to pre-CAR T cell neurologic baseline by day +7.

At dose level 2, patient 4 also experienced early and severe (grade 3) CAR neurotoxicity on day +1. The patient was initiated on

dexamethasone and anakinra on day +1, and a single dose of tocilizumab (anti-IL6R) was added on day +2 in the setting of grade 2 CRS and continued grade 3 neurotoxicity. The patient's mental status improved markedly by day +3 and returned to pre-CAR T cell neurological baseline by day +4. Patient 5 entered the study with considerable progression of multifocal tumor noted on the day -1 MRI scan. On day +1, the patient experienced grade 2 CAR neurotoxicity. The patient received only dexamethasone for supportive care, with neurotoxicity improving to grade 1 by day +2. However, on day +14, the patient presented in the setting of a dexamethasone taper with worsening fatigue, generalized muscle weakness and anorexia, each of which was grade 3 and lasted 8 d, 8 d and 14 d, respectively, meeting protocol-defined criteria for DLT. The patient's dexamethasone dose was increased with improvement of these toxicities to grade 2 or lower by day +28. Patient 6 had tumor progression involving the left midbrain and associated severe right-sided hemiparesis on the day of CAR T cell injection. On day +1, the patient developed acute worsening of chronic expressive aphasia and further increase in right-sided weakness that progressed to complete hemiplegia; the patient also developed aphasia on day +2, consistent with grade 2 CAR neurotoxicity, and was treated with dexamethasone and anakinra. His aphasia and ICE scores improved to baseline by day +3, but his dense hemiparesis continued. To optimize rehabilitation potential and reduce corticosteroid exposure, the patient received a single dose of bevacizumab (7.5 mg kg⁻¹ intravenously) on day +6 and was discharged on a dexamethasone taper. There was mild improvement in right leg strength but no improvement in right arm strength by the day +28 visit.

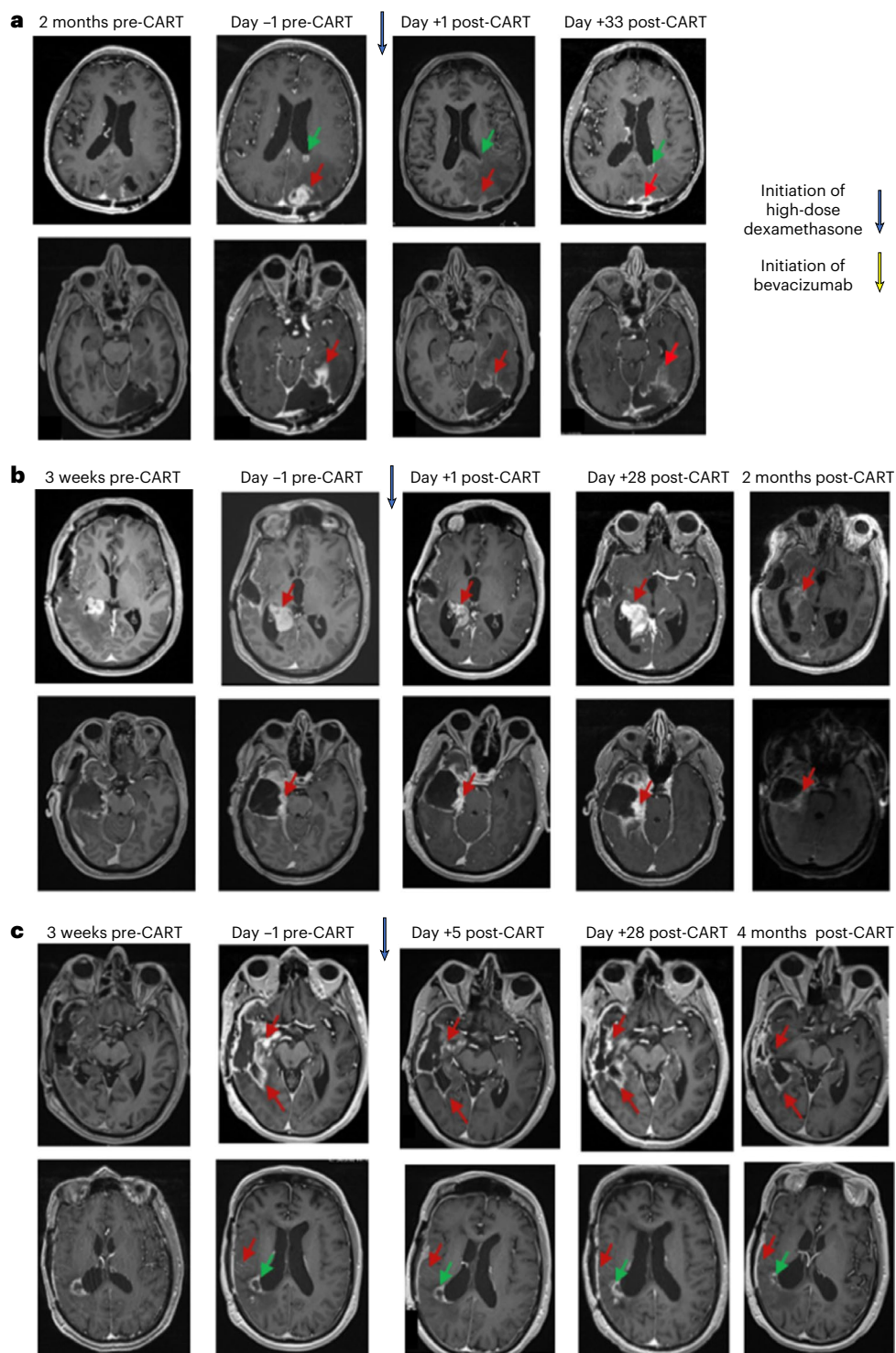
Preliminary efficacy

Reductions in the size of the enhancing tumor were observed in all six patients on the first MRI scan obtained 24–48 h after CAR T cell administration, with partial tumor regression maintained at day +28 and beyond in a subset of cases. However, none met criteria for an objective response per RANO criteria (Extended Data Table 2). Figure 1 (dose level 1) and Fig. 2 (dose level 2) display representative images from MRI scans obtained within the month before CAR T cell treatment and MRI scans obtained at pre-specified, protocol-defined imaging timepoints after CAR T cell treatment. Images are annotated with changes in dexamethasone dosage and use of bevacizumab over time. Tumor measurements by RANO criteria are provided in Extended Data Table 2. Of note, all patients were confirmed to have tumor progression histologically before receipt of CAR T cells and received no intervening anti-tumor therapies between the surgery confirming tumor progression histologically and receipt of CAR T cells. Moreover, all patients developed progressive, measurable tumor in the interim between surgical resection and receipt of CAR T cells. Longitudinal MRI findings and oncologic management/outcomes are described in detail for each patient in the subsequent sections.

In patient 1 (dose level 1), marked reduction of a large enhancing tumor nodule in the left parieto-occipital region was observed (Fig. 1a). On the patient's day +28 MRI scan (Fig. 1a), this nodule remained stable, but there was increased enhancement around the original left occipital operative cavity within the prior radiation field. The progressing area was then surgically resected, with pathology revealing mainly therapy-related changes and rare atypical glial cells constituting approximately 10% of the total cellularity. Targeted next-generation sequencing of the viable tumor component revealed no evidence of EGFR amplification or the patient's previously known EGFR extracellular domain mutation (Table 1). At 2 months after CAR T cell treatment, there was progression of disease with a separate, new focus of enhancing tumor in the left parietal lobe. The patient was eventually started on bevacizumab and remains alive with OS of 8 months from CAR T cell treatment at the time of this report. Patient 2 experienced reduction of a large enhancing tumor mass in the right mesial temporal lobe (Fig. 1b). Although the day +28 MRI scan showed an increase in size of the lesion,

Table 3 | All cohort 2 AEs that occurred after T cell administration and up to day 28

Category	Grades					Total
	1	2	3	4	5	
Toxicity						
Gastrointestinal disorders	6	0	0	0	0	6
Constipation	2	0	0	0	0	2
Flatulence	1	0	0	0	0	1
Nausea	1	0	0	0	0	1
Vomiting	2	0	0	0	0	2
General disorders and administration site conditions	2	1	1	0	0	4
Edema limbs	1	0	0	0	0	1
Fatigue	1	0	1	0	0	2
Hypothermia	0	1	0	0	0	1
Immune system disorders	1	2	0	0	0	3
CRS	1	2	0	0	0	3
Injury, poisoning and procedural complications	1	0	0	0	0	1
Fall	1	0	0	0	0	1
Investigations	8	4	1	0	0	13
Fibrinogen decreased	1	0	0	0	0	1
Hypokalemia	1	0	0	0	0	1
Hyponatremia	1	1	0	0	0	2
Hypophosphatemia	0	1	0	0	0	1
Investigations—other (lactic acid increased)	1	0	0	0	0	1
Lipase increased	0	2	0	0	0	2
Lymphocyte count decreased	0	0	1	0	0	1
Platelet count decreased	1	0	0	0	0	1
Serum amylase increased	3	0	0	0	0	3
Metabolism and nutrition disorders	2	0	1	0	0	3
Anorexia	0	0	1	0	0	1
Hypoalbuminemia	1	0	0	0	0	1
Hypophosphatemia	1	0	0	0	0	1
Musculoskeletal and connective tissue disorders	0	0	1	0	0	1
Generalized muscle weakness	0	0	1	0	0	1
Nervous system disorders	2	6	1	0	0	9
Dizziness	0	1	0	0	0	1
Dysphasia	0	1	0	0	0	1
Headache	0	1	0	0	0	1
Nervous system disorders—other (CAR neurotoxicity)	0	2	1	0	0	3
Seizure	1	0	0	0	0	1
Somnolence	0	1	0	0	0	1
Tremor	1	0	0	0	0	1
Renal and urinary disorders	1	2	0	0	0	3
Urinary incontinence	1	0	0	0	0	1
Urinary tract infection	0	1	0	0	0	1
Urinary urgency	0	1	0	0	0	1
Respiratory, thoracic and mediastinal disorders	0	1	1	0	0	2
Hypoxia	0	0	1	0	0	1
Voice alteration	0	1	0	0	0	1
Total	23	16	6	0	0	45



the 2-month MRI scan revealed that the tumor had regressed again in the absence of any intervening therapy (Fig. 1b), most consistent with resolving pseudo-progression. The patient then developed symptoms and radiographic evidence of communicating hydrocephalus shortly after the 2-month MRI scan. The patient declined intervention for shunting and elected for hospice care, eventually dying 5 months after CAR T cell treatment. In patient 3, the immediate post-CAR-T-cell MRI scan demonstrated decreased extent of nodular parenchymal enhancement in the right temporal lobe, decreased thickness of ependymal enhancement along the right lateral ventricle and near-complete resolution of previously seen leptomeningeal enhancement in the right hemispheric sulci (Fig. 1c). The patient continues to have stable disease

at the time of this report, including at the 4-month post-CAR-T-cell MRI scan (Fig. 1c).

At dose level 2, patient 4 experienced reduction of multiple foci of enhancement about the margins of the previous resection cavity, corpus callosum and left postcentral gyrus as well as reduction in enhancing periventricular nodules (Fig. 2a). The patient has continued to have stable disease at the time of this report, including on the most recent MRI scan performed at 3 months after CAR T cell treatment (Fig. 2a). Patient 5, who had displayed marked progression of tumor on the day -1 MRI scan relative to imaging 2 weeks earlier (Fig. 2b), also had early evidence for bioactivity. On the day +1 scan, there was substantial reduction in the extent of enhancement along the margins

Fig. 1 | Regression of multifocal rGBM after intraventricular delivery of CART-EGFR-IL13R α 2 cells (dose level 1). **a**, Patient 1. Compared to 2 months earlier, axial gadolinium-enhanced T1-weighted images obtained on day -1 demonstrated interval development of a solidly enhancing nodule in the left parieto-occipital region (top panel, red arrow) and a necrotic nodule bordering the ependyma of the left lateral ventricle (top panel, green arrow). There was regression of the dominant lesion -24 h after CAR T cell administration (top panel, red arrow). Repeat scan on day +33 demonstrated stable enhancement with slightly increased central necrosis at the site of the left parieto-occipital lesion (top panel, red arrow). However, there was increasing geographic enhancement at the left occipital resection cavity (bottom panel, red arrow). This area was then surgically resected with approximately 90% of the specimen revealing therapy-related changes. **b**, Patient 2. Day -1 images demonstrated a solidly enhancing posterior mesial temporal lobe nodule measuring 2.7 × 1.9 × 2.7 cm, substantially enlarged compared to 3 weeks earlier (top panel, red arrow). Reduction in size and avidity of enhancement was noted on day +1

(top panel, red arrow). Repeat images on day +28 demonstrated enlargement of the temporal nodule, now 5.4 × 4.1 × 3.1 cm (top panel, red arrow). Another MRI scan obtained 1 month later, without intervening therapy, demonstrated regression of the dominant nodule (2.8 × 1.4 × 2.5 cm) (top panel, red arrow). Thick enhancement at the medial margin of the resection cavity also increased on day +28 scan and remained stable to slightly regressed on the 2-month scan (bottom panel, red arrow). **c**, Patient 3. Compared to 3 weeks earlier, day -1 images showed increasing thick surrounding nodular enhancement extending into the mesial temporal lobe (top panel, red arrows). There was also linear sulcal enhancement (bottom panel, red arrow), concerning for leptomeningeal disease. Repeat imaging on day +2 demonstrated decreased nodular enhancement in the right temporal lobe (top panel, red arrows) and resolution of the linear sulcal enhancement (bottom panel, red arrow). At 4 months after CAR T cell treatment, images continued to demonstrate stability in the enhancement about the operative cavity (top panel, red arrows) and along the ependymal margin of the right temporal horn (bottom panel, green arrow). CART, CAR T cell treatment.

of the resection cavity as well as reduced tumor burden in the body and splenium of the corpus callosum (Fig. 2b). The patient was discharged to an acute rehabilitation facility but presented back to the hospital on day +14 with increasing lethargy, fatigue and poor oral intake in the setting of dexamethasone taper. MRI revealed increased enhancing signal abnormality about the resection cavity extending to the corpus callosum, fornix and ependyma, similar in appearance to the patient's immediate pre-CAR T cell treatment images (Fig. 2b). Steroid dosage was increased again with major clinical improvement. The patient's day +28 MRI scan then revealed marked interval decrease in the intensity of multifocal irregular enhancement, including the margins of the resection cavity and corpus callosum (Fig. 2b), potentially indicative of resolving pseudo-progression similar to that observed in patient 2. The patient had not yet undergone the 2-month MRI scan at the time of this report. Finally, in patient 6, who was experiencing tumor progression involving the left midbrain at the time of CAR T cell treatment (Fig. 2c), the day +1 MRI scan revealed less conspicuous enhancement with associated increasing central necrosis in the midbrain lesion and along the margins of the resection cavity as well as slight interval decrease in the nodular periventricular/ependymal enhancement at the left genu of the corpus callosum and in the left posterior lateral ventricle (Fig. 2c). The patient received a single intravenous dose of bevacizumab (7.5 mg kg⁻¹) on day +6 with subsequent improvement in right-sided strength. The day +28 MRI scan revealed stable disease (Fig. 2c), and the patient had not yet undergone the 2-month MRI scan at the time of this report.

Tumor target expression, pharmacokinetics and cytokines

In exploratory endpoint analyses, pre-treatment tumor tissue was stained via immunofluorescence for presence of both targets (Extended Data Fig. 3), and peripheral blood and cerebrospinal fluid (CSF) were

collected before CAR T cell administration on day 0 and on days 1, 4, 7, 10, 14, 21 and 28. To evaluate CAR T cell pharmacokinetics in the CSF, quantitative polymerase chain reaction (qPCR) and Luminex assays were performed as previously described⁷.

Peaks of CART-EGFR-IL13R α 2 cells in the CSF, likely indicative of level of engraftment and/or expansion and shown in other studies to be associated with clinical outcomes²³, were observed between days 1 and 7 and reached an average of 109,235 copies of CAR per microgram of genomic DNA (gDNA) (Fig. 3a). These levels are substantially higher than observed in our prior trials using peripheral blood infusion of CAR T cells for GBM (not exceeding 2,000 copies of CAR per microgram of gDNA in blood) and relatively similar to peaks observed in patients with hematologic malignancies treated with CD19-targeted CAR T cells²⁴. Notably, CART-EGFR-IL13R α 2 cells were also found in the peripheral blood in all patients (Fig. 3b), demonstrating communication between the CSF and peripheral blood compartments. In addition to CAR copies per microgram of DNA in CSF (Fig. 3c), engraftment data for CSF are also presented as CAR copies per milliliter of CSF to account for the varying cell counts and DNA quantities at different sample timepoints (Fig. 3d).

CSF cytokine levels supported evidence of CAR T cell activation and cytotoxic activity. IFN γ , IL-2, TNF α and IL-6, all markers of T cell activation, showed rapid increases in CSF before subsiding to baseline levels within 2 weeks (Fig. 3e), temporally consistent with preclinical data²⁵. Full cytokine data are presented in Supplementary Tables 4 and 5.

Discussion

GBM is an aggressive and highly treatment-refractory brain cancer. Clinically meaningful treatment options for relapsed disease after first-line radiotherapy are extremely limited, and no specific therapeutic intervention has ever been shown to prolong survival of patients

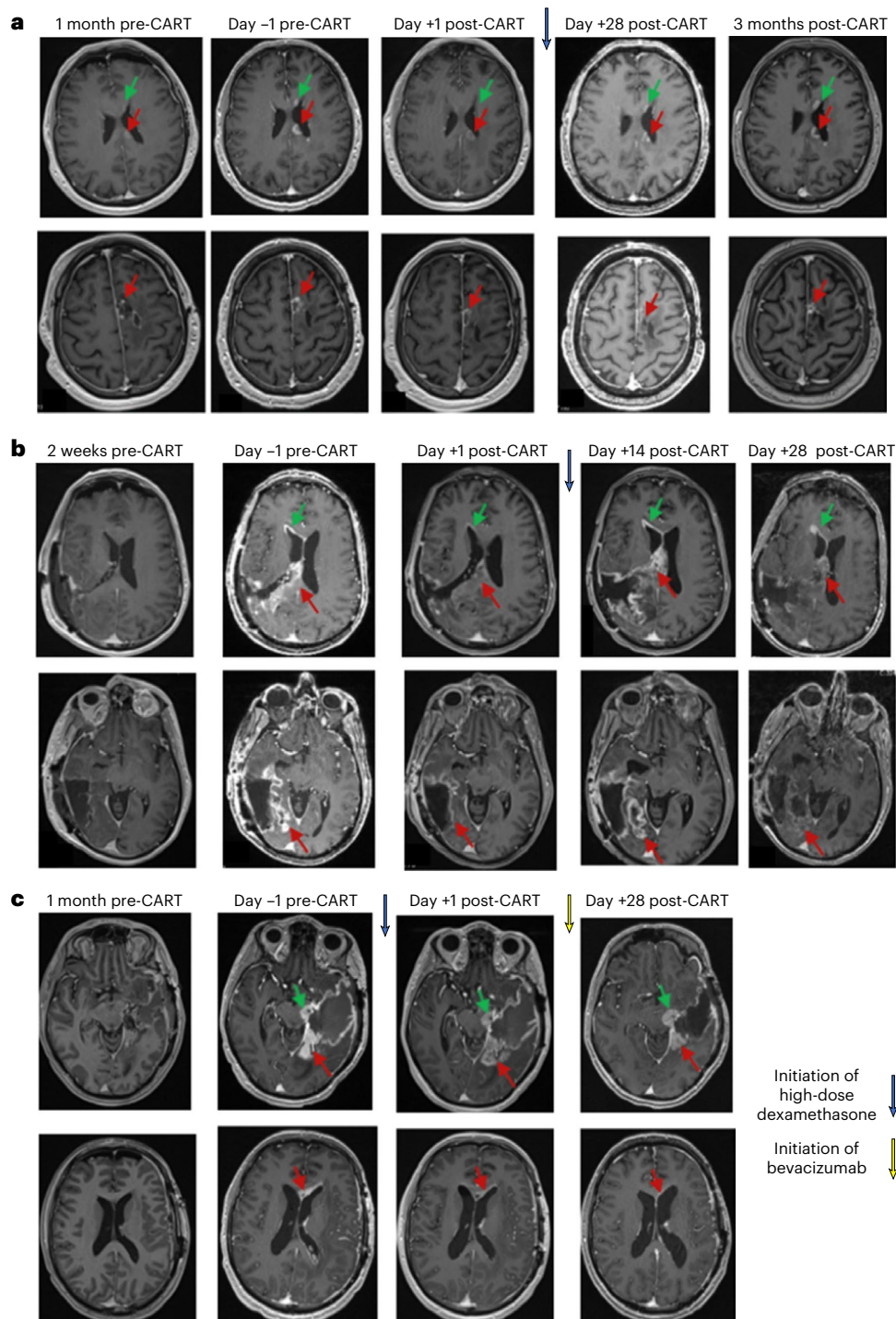
Fig. 2 | Regression of multifocal rGBM after intraventricular delivery of CART-EGFR-IL13R α 2 cells (dose level 2).

a, Patient 4. Axial gadolinium-enhanced T1-weighted images showed increased enhancing foci of disease on day -1, including in the corpus callosum (top panel, red arrow), along the ependymal surface of the left lateral ventricle (top panel, green arrow) and surrounding the left frontal resection cavity (bottom panel, red arrow). Day +1 images, obtained before any steroid administration, demonstrated reduction in all sites. The lesions were stable on day +28 and remained unchanged at the 3-month MRI timepoint. **b**, Patient 5. Compared to 2 weeks earlier, day -1 images demonstrated increasing irregular enhancement about the resection cavity (bottom panel, red arrow), extending along the right lateral ventricle into the corpus callosum (top panel, red arrow) and along the frontal horn (top panel, green arrow). Day +1 images, obtained before any steroid administration, showed reduction of tumor in the corpus callosum (top panel, red arrow) and right frontal horn (top panel, green arrow) as well as along the resection cavity (bottom panel, red arrow). These areas increased on a day +14 MRI scan obtained in the setting of

steroid taper and associated worsening lethargy but then improved by day +28 without intervening therapy other than an increase in steroids. **c**, Patient 6. Day -1 images showed tumor progression with increasing contrast-enhancing tumor at the left temporal resection cavity (top panel, red arrow), extension into the left midbrain (top panel, green arrow) and evidence of CSF dissemination at the left frontal horn (bottom panel, red arrow). Day +1 images revealed less conspicuous enhancement of the left midbrain lesion (top panel, green arrow), decreased enhancement and increased central necrosis at the posterior aspect of the resection cavity (top panel, red arrow) and reduced enhancement at the left frontal horn (bottom panel, red arrow). The patient received a single dose of bevacizumab on day +6, and day +28 imaging demonstrated stable disease, with continued decreases in the enhancement posterior to the resection cavity (top panel, red arrow) and left frontal horn (bottom panel, red arrow) but slight increase in size of the left midbrain lesion (top panel, green arrow). CART, CAR T cell treatment.

with rGBM. Here we report interim results of the first two dose levels of patients with rGBM treated on a phase 1 clinical trial of intrathecally delivered, autologous, bicistronic CAR T cells targeting EGFR epitope 806 and IL13R α 2. We observed early-onset acute neurotoxicity associated with administration of CART-EGFR-IL13R α 2 cells that was manageable at both dose levels (1×10^7 cells and 2.5×10^7 cells), and only one patient (dose level 2) experienced a protocol-defined DLT, which improved with increased dexamethasone dosage. It is notable that no grade 4 or grade 5 toxicities were observed. Although most elements of the observed neurotoxicity, including encephalopathy and depressed level of consciousness, were more typical of ICANS than T1AN²², the acute onset of neurological symptoms (12–24 h after CART T cell administration) and the lack of accompanying severe CRS

are notable differences from ICANS that have been well described in patients receiving cellular therapy for hematologic malignancies²⁶. Moreover, patient 1 experienced acute onset headache, nausea and vomiting that may have indicated elevated intracranial pressure, and patients 1, 2, 5 and 6 experienced acute worsening of chronic neurological deficits attributable to tumor location(s): all signs and symptoms potentially consistent with T1AN. In the setting of a potent and bioactive CAR T cell product delivered directly into the ventricular system, it is conceivable that patients may experience elements of both ICANS and T1AN. Larger numbers of treated patients and additional correlative work are needed to better characterize the neurotoxicity associated with CART-EGFR-IL13R α 2 cells and to develop optimal grading and management guidelines.



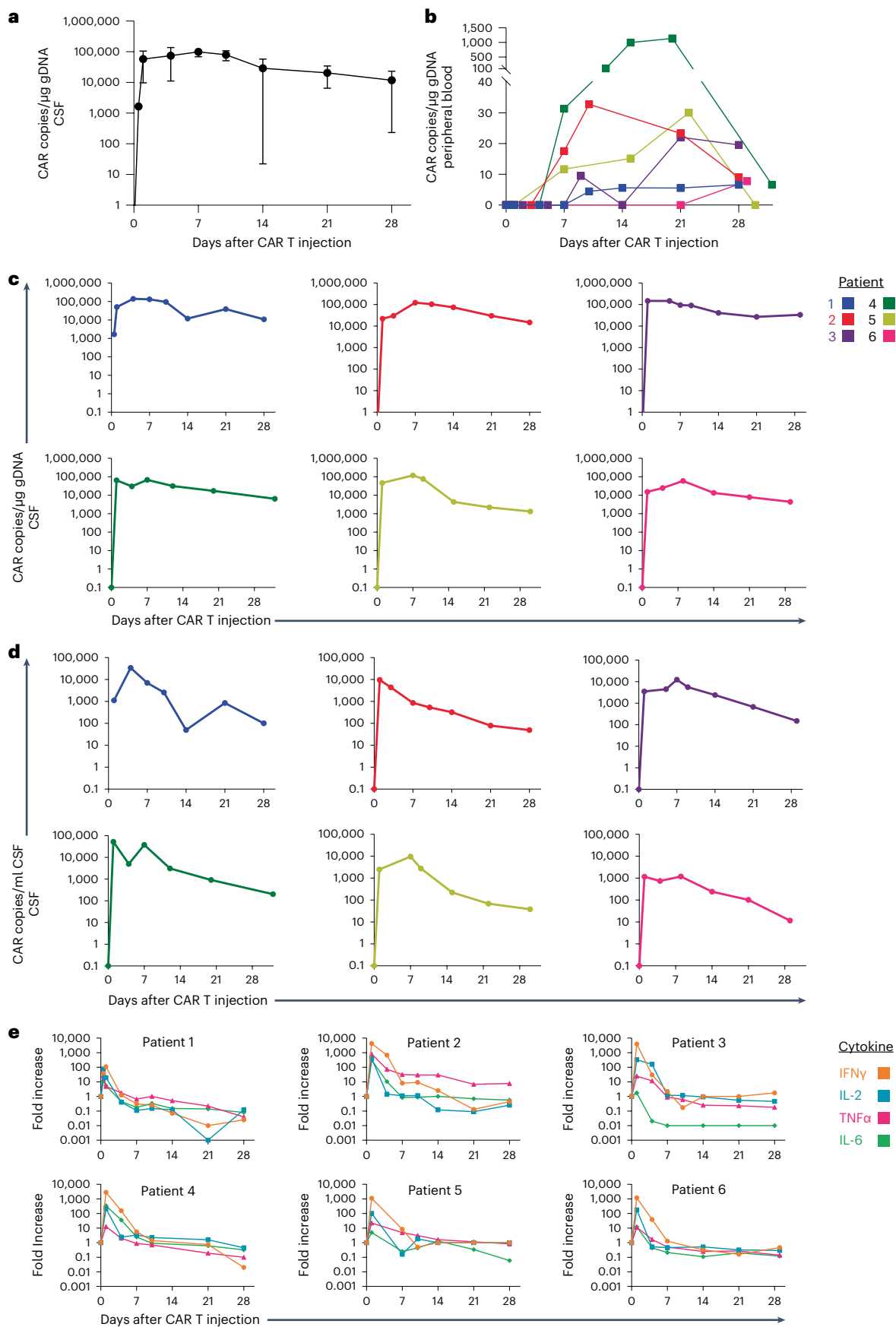


Fig. 3 | CAR T engraftment kinetics and CSF cytokine levels. **a**, Average levels of CAR T cells detected in the CSF after CAR T cell injection, using qPCR (copies per microgram of gDNA). Data presented are averaged values across all six patients \pm s.d. **b**, Individual patient levels of CAR T cells found in the peripheral blood. Positive signals in all six patients show communication of CAR T cells from the tumor or CSF into the peripheral circulation. Lower limit of quantification is 1 CAR copy per microgram of gDNA. **c**, Individual patient CAR T engraftment levels

in the CSF, through day +28 (copies per microgram of gDNA). All patients initiated high-dose dexamethasone between 10 h and 24 h after CAR T cell injection. **d**, CAR T cell engraftment kinetics in CSF as measured in CAR copies per milliliter of CSF. **e**, Individual patient CSF cytokine data for IFN γ , IL-2, TNF α and IL-6 showing peaks in the first 1–4 d after injection and returning to baseline by approximately 14 d. All patients initiated high-dose dexamethasone between 10 h and 24 h after CAR T cell injection.

Although the sample size treated thus far is small, and the follow-up duration is relatively brief, CART-EGFR-IL13R α 2 cells mediated reductions in enhancement and tumor size at early post-treatment timepoints in all six patients with multifocal, treatment-refractory rGBM. Although none met criteria for an objective response according to mRANO criteria (that is, \geq 50% decrease in the sum of products of perpendicular diameters of all measurable enhancing lesions sustained for at least 4 weeks), tumor shrinkage of at least 30% was observed in three of six patients, and stable disease was maintained on scans performed at least 2 months after CAR T cell therapy in three of the four patients who had at least 2 months of follow-up time, arguing against a ‘pseudo-response’ phenomenon. Although the effects on tumor enhancement and size were observed more quickly (that is, within 24–48 h) after CAR T cell injection than what is expected with other immunotherapies, such as immune checkpoint inhibitors, such rapid tumor cell killing is (1) consistent with intrathecally delivered CAR T cells coming into contact with tumor cells soon upon CSF entry and (2) occurring on a timeline that corresponds to the onset of neurotoxicity and peak CAR T cell and pro-inflammatory cytokine levels in the CSF. It is also notable that two patients experienced apparent pseudoprogression, with marked increases in enhancing tumor burden at the day +28 and day +14 timepoints, respectively, followed by substantial tumor regressions on short-term follow-up MRI scans in the absence of intervening anti-neoplastic therapy. Similar radiographic patterns of pseudoprogression were described in patients with non-Hodgkin’s B cell lymphoma treated with anti-CD19 CAR T cells²⁷ and in children with H3K27M-mutated diffuse midline gliomas after intrathecal administration of GD2-targeted CAR T cells²⁸. More complete characterization of this phenomenon will require treatment of additional patients along with serial tissue sampling when feasible.

These initial results from this ongoing phase 1 dose-escalation study have limitations, as only six patients have been treated, and follow-up time is relatively limited. Treatment of additional patients at dose level 2 and subsequent dose escalation or de-escalation are needed to better characterize the short-term and long-term safety profiles and optimal dose of CART-EGFR-IL13R α 2 cells. Of note, peak CAR T cell engraftment in the CSF was lower in patients who received the higher dose of CAR T cells at dose level 2 compared to patients treated at dose level 1. This raises an important question about whether increasing doses of CART-EGFR-IL13R α 2 cells may be detrimental to CAR T cell expansion, and this will be carefully evaluated as more patients are treated. In addition, the longer-term durability of stable disease induced by this therapy and effects on survival remain to be determined. It is also unclear whether efficacy may be enhanced by repeated locoregional delivery, as has been shown to be feasible and safe in children with diffuse intrinsic pontine glioma²⁹. Nonetheless, our promising early experience with CART-EGFR-IL13R α 2 cells in patients with multifocal disease sets the stage for further optimization of this approach for rGBM, an exceptionally challenging cancer with a survival of only 4–11 months². Additional correlative studies are also planned and will be described in future reports, including complete characterization of effector/memory T cell phenotypes in the infusion products and its association with clinical outcomes; single-cell sequencing of serial CSF samples to delineate the evolution of the CAR T cells and other immune cell populations over time; and analysis of pre-treatment and post-treatment tumor tissue when available to understand CAR T cell tumor infiltration and effects on the tumor microenvironment.

Online content

Any methods, additional references, Nature Portfolio reporting summaries, source data, extended data, supplementary information, acknowledgements, peer review information; details of author contributions and competing interests; and statements of data and code availability are available at <https://doi.org/10.1038/s41591-024-02893-z>.

References

- Wen, P. Y. et al. Glioblastoma in adults: a Society for Neuro-Oncology (SNO) and European Society of Neuro-Oncology (EANO) consensus review on current management and future directions. *Neuro Oncol.* **22**, 1073–1113 (2020).
- O’Rourke, D. M. et al. A single dose of peripherally infused EGFRvIII-directed CAR T cells mediates antigen loss and induces adaptive resistance in patients with recurrent glioblastoma. *Sci. Transl. Med.* **9**, eaaa0984 (2017).
- Goff, S. L. et al. Pilot trial of adoptive transfer of chimeric antigen receptor-transduced T cells targeting EGFRvIII in patients with glioblastoma. *J. Immunother.* **42**, 126–135 (2019).
- Ahmed, N. et al. HER2-specific chimeric antigen receptor-modified virus-specific T cells for progressive glioblastoma: a phase 1 dose-escalation trial. *JAMA Oncol.* **3**, 1094–1101 (2017).
- Brown, C. E. et al. Bioactivity and safety of IL13R α 2-redireceted chimeric antigen receptor CD8⁺ T cells in patients with recurrent glioblastoma. *Clin. Cancer Res.* **21**, 4062–4072 (2015).
- Brown, C. E. et al. Regression of glioblastoma after chimeric antigen receptor T-cell therapy. *N. Engl. J. Med.* **375**, 2561–2569 (2016).
- Lin, Q. et al. First-in-human trial of EphA2-redireceted CAR T-cells in patients with recurrent glioblastoma: a preliminary report of three cases at the starting dose. *Front. Oncol.* **11**, 694941 (2021).
- Liu, Z. et al. Safety and antitumor activity of GD2-specific 4SCAR-T cells in patients with glioblastoma. *Mol. Cancer* **22**, 3 (2023).
- Durgin, J. S. et al. Case Report: Prolonged survival following EGFRvIII CAR T cell treatment for recurrent glioblastoma. *Front. Oncol.* **11**, 669071 (2021).
- Alizadeh, D. et al. IFN γ is critical for CAR T cell-mediated myeloid activation and induction of endogenous immunity. *Cancer Discov.* **11**, 2248–2265 (2021).
- Choe, J. H. et al. SynNotch-CAR T cells overcome challenges of specificity, heterogeneity, and persistence in treating glioblastoma. *Sci. Transl. Med.* **13**, eabe7378 (2021).
- Bielamowicz, K. et al. Trivalent CAR T cells overcome interpatient antigenic variability in glioblastoma. *Neuro Oncol.* **20**, 506–518 (2018).
- Yin, Y. et al. Locally secreted BiTEs complement CAR T cells by enhancing killing of antigen heterogeneous solid tumors. *Mol. Ther.* **30**, 2537–2553 (2022).
- Thokala, R. et al. High-affinity chimeric antigen receptor with cross-reactive scFv to clinically relevant EGFR oncogenic isoforms. *Front. Oncol.* **11**, 664236 (2021).
- Gan, H. K., Burgess, A. W., Clayton, A. H. & Scott, A. M. Targeting of a conformationally exposed, tumor-specific epitope of EGFR as a strategy for cancer therapy. *Cancer Res.* **72**, 2924–2930 (2012).
- Jungbluth, A. A. et al. A monoclonal antibody recognizing human cancers with amplification/overexpression of the human epidermal growth factor receptor. *Proc. Natl Acad. Sci. USA* **100**, 639–644 (2003).

17. Reilly, E. B. et al. Characterization of ABT-806, a humanized tumor-specific anti-EGFR monoclonal antibody. *Mol. Cancer Ther.* **14**, 1141–1151 (2015).
18. Yin, Y. et al. Checkpoint blockade reverses anergy in IL13Rα2 humanized scFv based CAR T cells to treat murine and canine gliomas. *Mol. Ther. Oncolytics* **11**, 20–38 (2018).
19. Lassman, A. B. et al. Comparison of biomarker assays for EGFR: implications for precision medicine in patients with glioblastoma. *Clin. Cancer Res.* **25**, 3259–3265 (2019).
20. Newman, J. P. et al. Interleukin-13 receptor alpha 2 cooperates with EGFRvIII signaling to promote glioblastoma multiforme. *Nat. Commun.* **8**, 1913 (2017).
21. Ellingson, B. M., Wen, P. Y. & Cloughesy, T. F. Modified criteria for radiographic response assessment in glioblastoma clinical trials. *Neurotherapeutics* **14**, 307–320 (2017).
22. Mahdi, J. et al. Tumor inflammation-associated neurotoxicity. *Nat. Med.* **29**, 803–810 (2023).
23. Cappell, K. M. & Kochenderfer, J. N. Long-term outcomes following CAR T cell therapy: what we know so far. *Nat. Rev. Clin. Oncol.* **20**, 359–371 (2023).
24. Maude, S. L. et al. Chimeric antigen receptor T cells for sustained remissions in leukemia. *N. Engl. J. Med.* **371**, 1507–1517 (2014).
25. Good, C. R. et al. An NK-like CAR T cell transition in CAR T cell dysfunction. *Cell* **184**, 6081–6100 (2021).
26. Santomasso, B. D. et al. Management of immune-related adverse events in patients treated with chimeric antigen receptor T-cell therapy: ASCO guideline. *J. Clin. Oncol.* **39**, 3978–3992 (2021).
27. Danylesko, I. et al. Immune imitation of tumor progression after anti-CD19 chimeric antigen receptor T cells treatment in aggressive B-cell lymphoma. *Bone Marrow Transplant.* **56**, 1134–1143 (2021).
28. Majzner, R. G. et al. GD2-CAR T cell therapy for H3K27M-mutated diffuse midline gliomas. *Nature* **603**, 934–941 (2022).
29. Vitanza, N. A. et al. Intraventricular B7-H3 CAR T cells for diffuse intrinsic pontine glioma: preliminary first-in-human bioactivity and safety. *Cancer Discov.* **13**, 114–131 (2023).

Publisher's note Springer Nature remains neutral with regard to jurisdictional claims in published maps and institutional affiliations.

Springer Nature or its licensor (e.g. a society or other partner) holds exclusive rights to this article under a publishing agreement with the author(s) or other rightsholder(s); author self-archiving of the accepted manuscript version of this article is solely governed by the terms of such publishing agreement and applicable law.

© The Author(s), under exclusive licence to Springer Nature America, Inc. 2024

¹Division of Hematology/Oncology, Department of Medicine, University of Pennsylvania Perelman School of Medicine, Philadelphia, PA, USA.

²Glioblastoma Translational Center of Excellence, Abramson Cancer Center, University of Pennsylvania Perelman School of Medicine, Philadelphia, PA, USA.

³Department of Neurosurgery, University of Pennsylvania Perelman School of Medicine, Philadelphia, PA, USA.

⁴Center for Cellular Immunotherapies, University of Pennsylvania Perelman School of Medicine, Philadelphia, PA, USA.

⁵Department of Microbiology, University of Pennsylvania Perelman School of Medicine, Philadelphia, PA, USA.

⁶Department of Neuroscience, University of Pennsylvania Perelman School of Medicine, Philadelphia, PA, USA.

⁷Department of Radiology, University of Pennsylvania Perelman School of Medicine, Philadelphia, PA, USA.

⁸Kite Pharma, a Gilead Company, Santa Monica, CA, USA.

⁹Department of Pathology and Laboratory Medicine, University of Pennsylvania Perelman School of Medicine, Philadelphia, PA, USA.

¹⁰Department of Biostatistics, Epidemiology, and Informatics, University of Pennsylvania Perelman School of Medicine, Philadelphia, PA, USA.

¹¹Institute for Regenerative Medicine, University of Pennsylvania Perelman School of Medicine, Philadelphia, PA, USA.

¹²These authors contributed equally: Stephen J. Bagley, Meghan Logun, Zev A. Binder, Donald M. O'Rourke. ✉ e-mail: sbagley@pennmedicine.upenn.edu;

donald.orourke@pennmedicine.upenn.edu

Methods

Protocol development and study monitoring

The study protocol has undergone five amendments since its original version (version 1, 15 November 2021) and is currently in version 6 (18 January 2024). These are displayed in the Study Protocol provided in the Supplementary Information.

An independent data safety monitoring board was chartered for this study and meets on a semiannual basis to review SAEs and suspected unexpected SAEs.

Clinical vector manufacturing

The bicistronic CART-EGFR-IL13R α 2 vector encodes two CAR transgenes that recognize either the EGFR epitope 806 (ref. 14) or IL13R α 2 (ref. 18). Both transgenes were expressed from the same transcript using P2A, the 2A self-cleaving mechanism of porcine teschovirus. The CAR sequences were cloned into a third-generation self-inactivating lentiviral expression vector containing the EF-1 α promoter, a cPPT sequence, a Rev response element and a woodchuck hepatitis virus post-transcriptional regulatory element (WPRE). Plasmid DNA was generated by Puresyn, Inc. Lentiviral vector was produced via transient transfection with four plasmids expressing the transgene, RSV-Rev, VSV-G and gag-pol in human embryonic kidney 293T cells at the University of Pennsylvania Center for Advanced Retinal and Ocular Therapeutics Vector Core.

Leukapheresis procedure

A large-volume apheresis procedure was carried out at the Hospital of the University of Pennsylvania apheresis center according to standard clinical procedures. Peripheral blood mononuclear cells (PBMCs) were obtained for CAR T cells during this procedure. From a single leukapheresis, the intention was to harvest at least 5×10^9 white blood cells to manufacture CAR T cells. If the apheresis does not yield an adequate number of cells required for manufacturing or the T cell manufacture is unsuccessful, patients can undergo an additional apheresis as needed. It is recommended that the patient have an absolute lymphocyte count (ALC) ≥ 500 per microliter before undergoing apheresis. If the patient's ALC is less than 500 per microliter, it is recommended that a lymphocyte subset analysis (CD3, CD4 and CD8 counts) be performed to confirm that the patient has an absolute CD3 count of ≥ 150 per microliter. If the absolute CD3 count is less than 150 per microliter, it is recommended that the leukapheresis procedure be delayed until their ALC is ≥ 500 per microliter or until absolute CD3 count is ≥ 150 per microliter.

T cell manufacturing

CART-EGFR-IL13R α 2 was manufactured by the Clinical Cell and Vaccine Production Facility at the University of Pennsylvania. In brief, autologous peripheral blood lymphocytes were collected via leukapheresis. On day 0, cryopreserved leukapheresis material was thawed and washed, followed by enrichment for CD4⁺ and CD8⁺ T cells using immunomagnetic microbeads (CliniMACS, Miltenyi Biotec). Enriched CD4/CD8 cells were then activated with anti-CD3/anti-CD28 monoclonal antibody (mAb)-coated paramagnetic beads (Dynabeads CD3/CD28 CTS, Thermo Fisher Scientific). Cells were transduced with the bicistronic CART-EGFR-IL13R α 2 lentiviral vector on day 1, after which the culture continued expansion in media (Life Technologies) supplemented with IL-7 and IL-15 (MACS GMP Products, Miltenyi Biotec) through harvest days 9–11. At the conclusion of the culture period, cells were washed using a closed system washing device, depleted of magnetic beads and formulated in infusible cryopreservation media (BioLife Solutions). The final CAR T product was frozen using a controlled-rate freezer and stored in a monitored freezer in vapor phase liquid nitrogen (LN). Full product release testing was completed before release of the product.

Infusion product characterization

Before product harvest, a sample was tested for scFv expression by flow cytometry. The cells were stained with the biotin-conjugated goat

anti-mouse IgG (Jackson ImmunoResearch) followed by PE-labeled streptavidin as well as mAbs specific to CD3 (BD Biosciences), CD45 (BD Biosciences) and Via-Probe (BD Biosciences) in FACS buffer. The cells were acquired on the NovoCyte Quanteon flow cytometer (Agilent) and analyzed with the dedicated software. Cells were gated on the live population, singlets and double CD45CD3 positive, and the EGFR scFv expressing cells were displayed; the percent of EGFR CAR positive was reported on the product Certificate of Analysis for product release. The IL13R α 2 expression was determined for information only using the same CD3, CD45 and viaprobe reagents as well as the human IL-13R α 2 His-tagged protein (Sino Biological) followed by the His-tag APC-conjugated antibody (R&D Systems).

Separately, the phenotype of the harvest product was analyzed by staining a sample with mAbs specific to CD3, CD4, CD8 and CD45 (BD Biosciences and BioLegend). The cells were acquired on the NovoCyte Quanteon flow cytometer (Agilent) and analyzed with the dedicated software. Cells were gated on live singlets, followed by various marker combinations. The percentages of CD45/CD3/CD4 and CD45/CD3/CD8 positive populations were determined, and their ratio was calculated.

Patient eligibility

Inclusion criteria.

1. Signed, written informed consent
2. Male or female age ≥ 18 years of age
3. Patients with glioblastoma, IDH wild-type (as defined by the World Health Organization 2021 Classification of CNS Tumors), that has recurred after prior radiotherapy². For patients with tumors harboring methylation of the *MGMT* promoter, at least 12 weeks must have elapsed since completion of first-line radiotherapy.
4. Tumor tissue positive for wild-type EGFR amplification by NeoGenomics Laboratories (FISH analysis) was used. A sample is considered positive for EGFR amplification if one of the following four criteria are met: (1) EGFR/CEN7 ≥ 2.0 , (2) clusters of ≥ 4 EGFR signals per cell in $\geq 10\%$ of tumor cells, (3) ≥ 4 EGFR signals per cell present in $\geq 40\%$ of tumor cells or (4) ≥ 15 EGFR signals per cell present in $\geq 10\%$ of tumor cells. Archival tumor from patient's initial surgery at time of original diagnosis or recently collected tumor from time of recurrence are acceptable.
5. Surgical tumor resection for disease control/management or tumor biopsy to confirm tumor recurrence is clinically indicated in the opinion of the physician-investigator.
6. Adequate organ function is defined as:
 - a. Serum creatinine $\leq 1.5 \times$ the upper limit of normal (ULN) or estimated creatinine clearance ≥ 30 ml min⁻¹ and not on dialysis
 - b. Alanine transaminase (ALT)/aspartate transaminase (AST) $\leq 3 \times$ ULN range and total bilirubin ≤ 2.0 mg dl⁻¹, except for patients in whom hyperbilirubinemia is attributed to Gilbert's syndrome (≤ 3.0 mg dl⁻¹)
 - c. Left ventricular ejection fraction (LVEF) $\geq 45\%$ confirmed by ECHO/MUGA
 - d. Must have a minimum level of pulmonary reserve defined as \leq grade 1 dyspnea and pulse oxygen $>92\%$ on room air
7. Karnofsky Performance Status (KPS) $\geq 60\%$
8. Patients of reproductive potential must agree to use acceptable birth control methods.

Exclusion criteria.

1. Active hepatitis B or hepatitis C infection
2. Any other active, uncontrolled infection
3. Class III/IV cardiovascular disability according to the New York Heart Association classification
4. Tumors primarily localized to the brain stem or spinal cord

5. Severe, active comorbidity that, in the opinion of the physician-investigator, would preclude participation in this study
6. Receipt of bevacizumab within 3 months before physician-investigator confirmation of eligibility
7. Active autoimmune disease requiring systemic immunosuppressive treatment equivalent to ≥ 10 mg daily of prednisone. Patients with autoimmune neurological diseases (such as multiple sclerosis or Parkinson's disease) are excluded.
8. Pregnant or nursing (lactating) women
9. History of allergy or hypersensitivity to study product excipients (human serum albumin, dimethyl sulfoxide (DMSO) and Dextran 40)

Administration of CART-EGFR-IL13R α 2 cells

CART-EGFR-IL13R α 2 cells were released in a CellSeal Cryovial and thawed using the CellSeal Vial Automatic Thawing System. Once the cell product was thawed, the entire contents of the cryovial were withdrawn into a syringe using a sterile adapter. CART-EGFR-IL13R α 2 cells were then delivered via intrathecal administration through the patient's Ommaya reservoir using a small-gauge needle with accompanying non-filtered tubing, connected to a stopcock and sterile 5–10-ml syringes. Cells were injected at a rate of approximately 1 ml min⁻¹.

Definition of DLT

AEs were graded according to the National Cancer Institute Common Terminology Criteria for Adverse Events, version 5.0. The DLT observation period was 28 d after initial treatment with CART-EGFR-IL13R α 2 cells (day 0). To allow for appropriate monitoring and assessment of toxicities, the CART-EGFR-IL13R α 2 injections in the 1st and 2nd patients in each cohort were staggered by ≥ 28 d.

A DLT was defined as any of the following occurring within 28 d after initial CART-EGFR-IL13R α 2 cell administration (day 0):

- CRS: grade 4 CRS that fails to improve to \leq grade 3 within 72 h or grade 3 CRS that fails to improve to \leq grade 2 within 7 d of first onset
- CAR neurotoxicity (by the Penn modified grading criteria for CAR neurotoxicity in patients with GBM): any grade 4 CAR neurotoxicity; any grade 3 CAR neurotoxicity that fails to improve to \leq grade 2 after 72 h and is not an obvious direct result of tumor progression as jointly determined by the medical director and the principal investigator
- Non-hematologic toxicities*:
 - Any grade 4 non-hematologic event, unless clearly related to causes other than the CART-EGFR-IL13R α 2 cells
 - Any grade 3 event that does not resolve to \leq grade 2 or baseline within 7 d, unless clearly related to causes other than the CART-EGFR-IL13R α 2 cells
- Hematologic toxicities:
 - Grade 4 neutropenia or thrombocytopenia that does not resolve to at least grade 3 within 14 d after the CART-EGFR-IL13R α 2 injection
 - Grade 4 anemia
- Any $>$ grade 3 possibly and probably related to the CSF ventricular reservoir
- Any treatment-related death

*Component events that are captured as AEs of particular interest (such as hypoxia and hypotension in the setting of CRS) may not be evaluated separately against the DLT definition.

Patient sample processing and analysis

Whole blood from the patients was processed using a Ficoll gradient. PBMCs were stored in RPMI 1640 media (Gibco) with 10% DMSO

and 20% FBS (Gemini BioProducts) and kept in LN until later use. CSF samples were processed to obtain supernatant and cell pellet. The supernatant was frozen and kept at -80 °C until later use. The pellet was used to isolate DNA. Quantification of transgene in the peripheral blood and CSF was performed using real-time quantitative polymerase chain reaction (qRT-PCR), as described previously². In brief, research sample processing, freezing and qRT-PCR were performed in the Translational and Correlative Studies Laboratory at the University of Pennsylvania, using established standard operating procedures (SOPs). CAR T cells were quantified from peripheral blood, and CSF samples were obtained at protocol-specified timepoints. Peripheral blood samples were collected in lavender top (K2EDTA) Vacutainer tubes (Becton Dickinson), and CSF samples were collected in sterile syringes. All samples were delivered to the laboratory within 2 h of acquisition and processed within 16 h of acquisition, according to established SOPs. gDNA was isolated directly from whole blood and CSF cell pellet, and qRT-PCR analysis was performed using ABI TaqMan technology to detect the integrated CAR transgene sequence, using triplicates of 200 ng of gDNA (or maximum available) per timepoint for patient samples. To determine copy number per unit of DNA, an eight-point standard curve was generated consisting of up to 1×10^6 copies of lentivirus plasmid spiked into 200 ng of non-transduced control gDNA. The number of copies of plasmid present in the standard curve was verified using digital qRT-PCR with the same primer/probe set and performed on a QIAcuity One (Qiagen). For quality control checks, each datapoint (sample and standard curve) was evaluated in triplicate with a positive C_t value in three of three replicates. Additionally, the acceptable percent coefficient of variation was less than 0.95% for all quantifiable values. To control for the quantity of interrogated DNA, we performed a parallel amplification reaction using 10 ng of gDNA and a primer/probe combination specific for a non-transcribed genomic sequence upstream of the CDKN1A (p21) gene. These amplification reactions generated a correction factor to adjust for calculated versus actual DNA input. Copies of transgene per microgram of DNA were calculated according to the following formula: copies per microgram of gDNA = (copies calculated from CAR T standard curve) \times correction factor / (amount DNA evaluated in nanograms) \times 1,000 ng. In patient 1, the baseline CSF sample (obtained on day 0 before CAR T cell injection) was contaminated with CAR T cell infusion product due to the CSF sample coming into contact with the infusion product via the three-way stopcock used during injection. This sample was, therefore, excluded from the engraftment analysis displayed in Fig. 2c. For patient 1, the first timepoint shown in the qPCR CSF plot is 10 h after CAR T cell injection, as this patient had an unscheduled CSF draw in the setting of neurotoxicity soon after CAR T cell injection.

Because (1) expressing the CSF data as CAR copies per microgram of DNA assumes a constant DNA amount per reaction and (2) the amount of DNA obtained from CAR T cells in CSF is variable at different samples given the low cell counts in samples at certain timepoints, we also expressed the CSF engraftment data as CAR copies per milliliter of CSF. This ensures consistent measurement from the CSF despite varying cell counts/DNA quantities at some sample timepoints. Initial CSF volumes for correlative analysis were recorded, ranging from 2 ml to 4.75 ml. After centrifugation of the CSF samples, the entire cell pellet from each sample was used for DNA isolation, with a uniform volume of 90 μ l of eluted DNA across all samples. The concentration of this DNA was measured in nanograms per microliter (ng μ l⁻¹) using a standard curve-based p21 qPCR assay (see above). To determine the number of cells per microliter from this DNA concentration, a formula was applied where the DNA concentration from the p21 assay was divided by 0.0064 ng—the weight of gDNA from a single cell. The proportion of CAR T cells within each microliter was then ascertained by multiplying the cell number by the average copy number per cell from the transgene-specific qPCR assay. This figure, representing the number of CAR T cells per microliter, was further multiplied by 90 μ l to reflect

the total CAR T cells in the isolated DNA volume. The final concentration of CAR T cells in the original CSF was then determined by dividing this total by the initial CSF volume, thus providing the concentration of CAR T cells per 1 ml of CSF.

Serum and CSF supernatant samples collected before and after CAR T cell injection initially cryopreserved at -80°C were thawed and analyzed for multiplex cytokine measurements using a custom 32-plex human cytokine panel from EMD Millipore. The following analytes were included in the panel: EGF, FGF-2, eotaxin, sIL-2Ra, G-CSF, GM-CSF, IFN- α 2, IFN- γ , IL-10, IL-12P40, IL-12P70, IL-13, IL-15, IL-17A, IL-1RA, HGF, IL-1 β , CXCL9/MIG, IL-2, IL-4, IL-5, IL-6, IL-7, IL-18, CXCL8/IL-8, CXCL10/IP-10, CCL2/MCP-1, CCL3/MIP-1 α , CCL4/MIP-1 β , RANTES, TNF- α and VEGF. All samples were analyzed in duplicate according to the manufacturer's instructions and compared against multiple internal standards with a six-point standard curve. Data were acquired on a FlexMAP-3D system (Luminex), and analysis was performed using XPonent 4.3 software (Luminex). In the event that samples returned low out-of-range values, the following equation was used to approximate baseline readings, as done previously²⁴:

$$\frac{\text{Standard curve minimum} \times \text{Dilution Factor}}{2}$$

Clinical imaging

Brain MRI was performed in all patients on a 3T magnet (Magnetom Skyra, Magnetom Vida Siemens) including volumetric axial T1-weighted 3D MPRAGE (TR/TE/TI = 2,200/2.4/900 ms, 192×256 matrix size, 1-mm section thickness) before and after contrast as well as axial FLAIR (TR/TE/TI = 10,060/133/2,550 ms, 3-mm section thickness).

Immunofluorescence methods

Sections of patient tumor resection material were collected and sectioned according to clinical protocol by the University of Pennsylvania's Department of Pathology. Staining was performed on 5-mm sections of formalin-fixed paraffin-embedded specimens after treatment with xylene and Pharmingen Retrieval A solution (BD Biosciences) for wax removal and antigen retrieval. Tissue sections were permeabilized and blocked using a solution of 10% donkey serum (v/v), 0.5% Triton X-100 (v/v), 1% BSA (w/v), 0.1% gelatin (w/v) and 22.52 mg ml⁻¹ glycine in TBST for 1 h at room temperature. Sections were incubated with primary antibodies (anti-EGFRvIII 806, Absolute Antibody, Ab03036-23.0; anti-IL13Ra2, R&D Systems, AF146) diluted in TBST with 5% donkey serum (v/v) and 0.1% Triton X-100 (v/v) overnight at 4 $^{\circ}\text{C}$. After washing in TBST, tissue sections were incubated with secondary antibodies diluted in TBST with 5% donkey serum (v/v) and 0.1% Triton X-100 (v/v) for 1.5 h at room temperature. After washing in TBST, sections were incubated with NucBlue reagent (Invitrogen) diluted in TBS for 10 min to stain cell nuclei. After washing with TBS, slides were mounted in mounting solution (eBioscience), cover slipped and sealed with nail polish.

Flow cytometry methods

Patient CAR T cell product provided by the Clinical Cell and Vaccine Production Facility was thawed at 37 $^{\circ}\text{C}$ and resuspended in PBS with 2% FBS for identification of CAR⁺ populations. Cells were incubated with biotinylated EGFRvIII protein (R&D Systems) or Fc-tagged IL13Ra2 protein (R&D Systems) for 30 min at 4 $^{\circ}\text{C}$ before staining with respective secondary antibodies for another 30 min at 4 $^{\circ}\text{C}$. Data acquisition was performed on an LSRFortessa Cell Analyzer (BD Biosciences) and analyzed using FlowJo 10.8.1 software.

Statistics

The statistical analysis for clinical data was primarily descriptive in keeping with the small sample size, 3 + 3 dose escalation design and interim nature of this report. No data were excluded from the analyses, and the correlative experiments were not randomized. No adjustments were made for multiple comparisons. The investigators were

not blinded to allocation during experiments and outcome assessment. Data distribution was assumed to be normal, but this was not formally tested. $P < 0.05$ was considered significant. All statistical tests described were two-sided and performed using R version 4.1.2 (R Foundation for Statistical Computing). Figures were generated using GraphPad Prism version 10.1 software.

Reporting summary

Further information on research design is available in the Nature Portfolio Reporting Summary linked to this article.

Data availability

The data that support the findings of this study are included in the paper or may be available from the corresponding author, recognizing that certain patient-related data not included in the paper were generated as part of the clinical trial and may be subject to patient confidentiality. It is estimated that the corresponding author will respond to external data requests within 2 weeks of receipt of request. Further information on research design is available in the Nature Research Reporting Summary linked to this article. Source data are provided with this paper.

Acknowledgements

The authors would like to thank the patients who participated in this study and their families for their dedication to furthering GBM treatment. The authors also thank the Neurosurgery Clinical Research Division, the Translational and Correlative Sciences Laboratory and the Clinical Cell and Vaccine Production Facility at the University of Pennsylvania Perelman School of Medicine for all of their clinical trial contributions and support. This work was funded by Kite Pharma (a Gilead company), the Abramson Cancer Center Glioblastoma Translational Center of Excellence to D.M.O., the Templeton Family Initiative in Neuro-Oncology to D.M.O., the Maria and Gabriele Troiano Brain Cancer Immunotherapy Fund to D.M.O., National Institutes of Health grants R35NS116843 to H.S. and R35NS097370 to G.-L.M. and the Dr. Miriam and Sheldon G. Adelson Medical Research Foundation to G.-L.M. Kite Pharma had an advisory role in the design of the study and review of the final manuscript but had no role in data collection, analysis, decision to publish or preparation of the manuscript.

Author contributions

Study design: S.J.B., A.S.D., E.M., L.L., A.M., R.L., J.K.J., S.C., B.S.O., G.P., A.B., W.G., D.B., W.-T.H., E.O.H., Z.A.B. and D.M.O. Patient recruitment and treatment: S.J.B., A.S.D., R.M. and E.M. Data generation, curation and analyses: S.J.B., M.L., J.A.F., X.W., A.S.D., L.J.B., A.N., D.J., R.M., C.S., R.L., J.K.J., S.C., V.G., F.C., Y.S., M.P.N., W.-T.H., G.-L.M., H.S., D.L.S., E.O.H., Z.A.B. and D.M.O. Writing—original draft: S.J.B. and Z.A.B. Writing—review and editing: S.J.B., C.H.J., E.O.H., Z.A.B. and D.M.O. Supervision: S.J.B., E.M., L.L., C.S., G.P., A.B., H.S., D.L.S., C.H.J., E.O.H., Z.A.B. and D.M.O. Funding support: W.G. and D.B.

Competing interests

S.J.B. has received consulting fees from Telix, Servier, Kiyatec, Novocure and Bayer and has received research funding from Kite Pharma (a Gilead company) related to the submitted work and from Incyte, Novocure, GSK and Eli Lilly, all outside of the submitted work. J.A.F. is a member of the scientific advisory boards of Cartography Bio and Shennon Biotechnologies and has patents, royalties and other intellectual property (IP). W.G. is an employee of Kite Pharma (a Gilead company). D.B. is an employee of Kite Pharma (a Gilead company). D.L.S. holds founder's equity and has licensed IP to Verismo Therapeutics and Vetigenics and has IP licensing to Chimeric Therapeutics. C.H.J. and the University of Pennsylvania have patents pending or issued related to the use of gene modification in T cells for adoptive T cell therapy. C.H.J. is a co-founder of Tmunity (acquired

by Kite Pharma, a Gilead company); is a scientific co-founder and holds equity in Capstan Therapeutics, Dispatch Biotherapeutics and BlueWhale Bio; serves on the board of AC Immune; is a scientific advisor to BlueSphereBio, Cabaletta, Carisma, Cartography, Cellares, Cellcarta, Celldex, Danaher, Decheng, ImmuneSensor, Kite Pharma, Poseida, Verismo, Viracta, Vittoria Biotherapeutics and WIRB-Copernicus group; and is an inventor on patents and/or patent applications licensed to Novartis Institutes of Biomedical Research and Kite Pharma and may receive license revenue from such licenses. Z.A.B. has inventorship interest in IP owned by the University of Pennsylvania and has received royalties related to CAR T therapy in solid tumors. D.M.O. reports prior or active roles as consultant/scientific advisory board member for Celldex Therapeutics, Prescient Therapeutics, Century Therapeutics and Chimeric Therapeutics and has received research funding from Celldex Therapeutics, Novartis, Tmunity Therapeutics and Gilead Sciences/Kite Pharma. D.M.O. is an inventor of IP (US patent numbers 7,625,558 and 6,417,168 and related families) and has received royalties related to targeted ErbB therapy in solid cancers previously licensed by the University of Pennsylvania. D.M.O. is also an inventor on multiple patents related to CAR T cell therapy in solid tumors that have been licensed by the University

of Pennsylvania and has received royalties from these license agreements. The remaining authors declare no competing interests.

Additional information

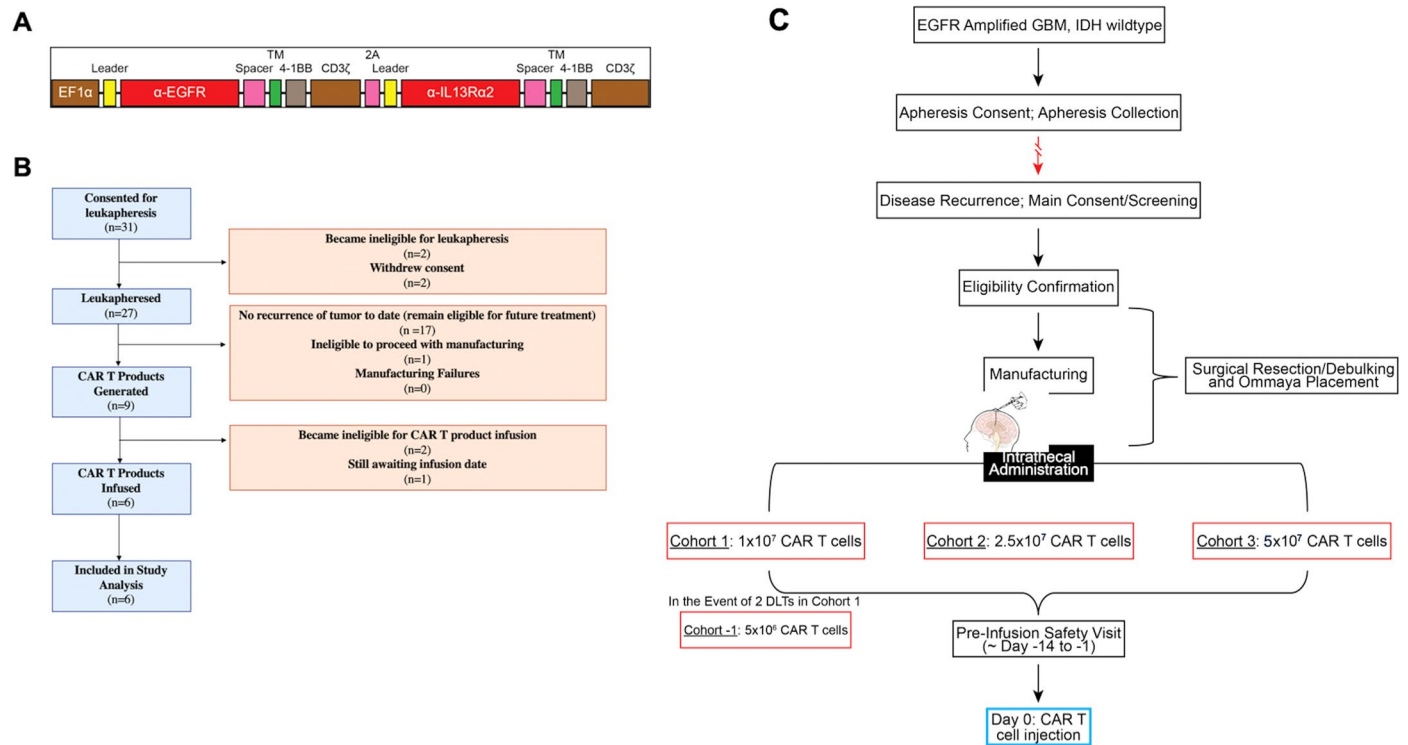
Extended data is available for this paper at <https://doi.org/10.1038/s41591-024-02893-z>.

Supplementary information The online version contains supplementary material available at <https://doi.org/10.1038/s41591-024-02893-z>.

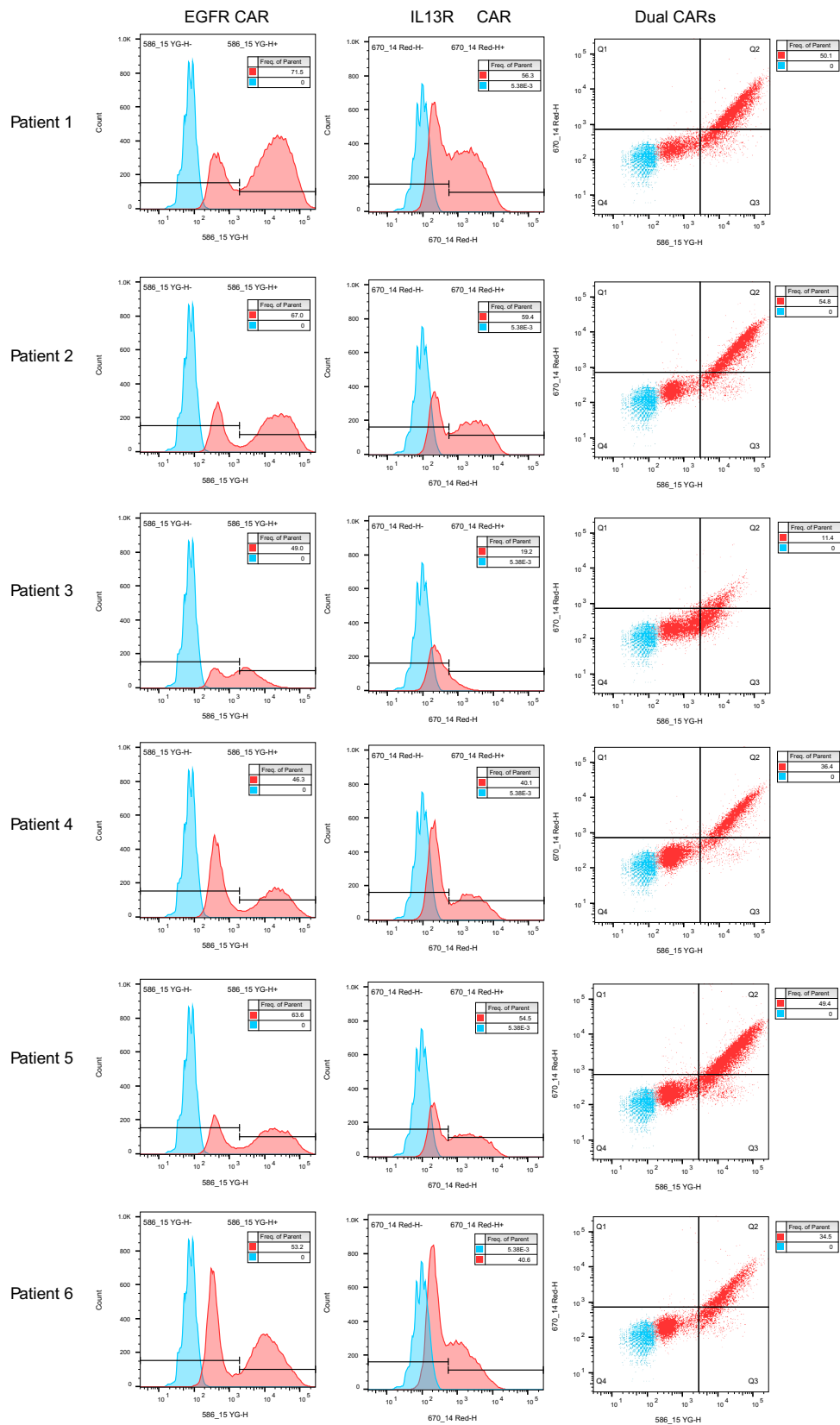
Correspondence and requests for materials should be addressed to Stephen J. Bagley or Donald M. O'Rourke.

Peer review information *Nature Medicine* thanks the anonymous reviewers for their contribution to the peer review of this work. Primary Handling Editor: Saheli Sadanand, in collaboration with the *Nature Medicine* team.

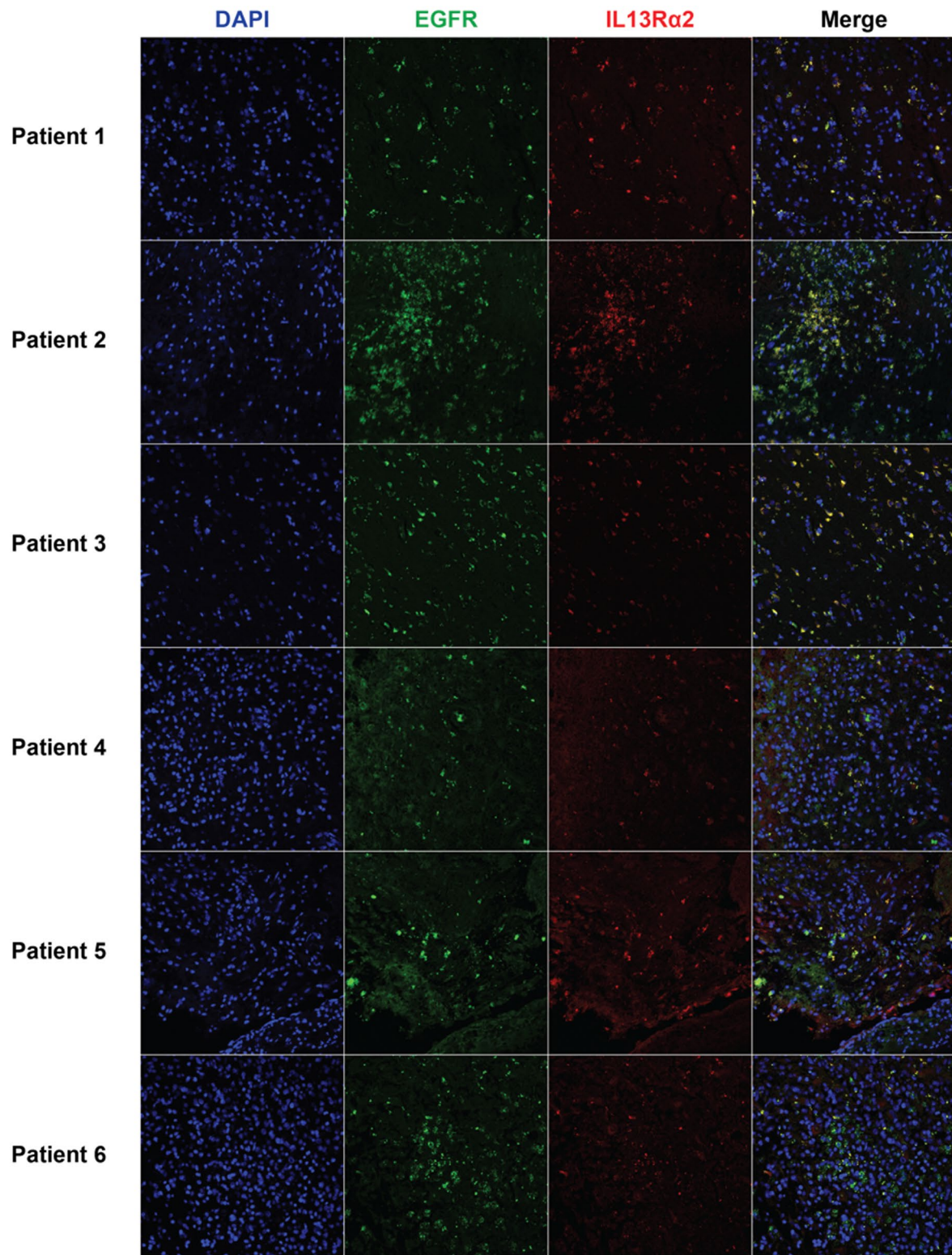
Reprints and permissions information is available at www.nature.com/reprints.



Extended Data Fig. 1 | CART-EGFR-IL13Rα2 construct, CONSORT diagram, and study schema. (a) The illustration depicts two parallel CARs with 4-1BB ζ intracellular signaling domains. **(b)** CONSORT flow diagram for the patients included in this report. **(c)** Study schema.



Extended Data Fig. 2 | Flow cytometry plots of optimized CAR detection assay. For each patient, histograms depict EGFR CAR (left column) and IL13R CAR (center column) expression. Dual CAR expression is quantified in dot plots (right column). CAR expression values in patient infusion products based on these flow cytometry plots are displayed in Supplementary Table 1.



Extended Data Fig. 3 | Immunofluorescence staining of EGFR CAR and IL13Ra2 CAR targets in patient pre-infusion tumor tissue. Tumor tissue obtained at the time of Ommaya placement was stained for both CAR targets.

All 6 patients treated demonstrated expression of one or both targets throughout their tumor. All images taken at 20x magnification. Staining was performed in duplicate. Scale bar = 100 μm .

Extended Data Table 1 | Individual patient CAR T cell product information

Patient	Dose Level	CART-EGFR-IL13R α 2 Target Cell Dose	Total Cell Dose	Volume for Injection	Days between surgery and CAR T cell injection	Cell Viability	%CD3 ⁺ CD45 ⁺	%scFv (EGFR)	%scFv (IL13R α 2)	Vector DNA Sequence (avg copies/cell)	CD4:CD8
1	1	1x10 ⁷	2.31x10 ⁷	2mL	29	92.9	99.3	43.4	12.4	1.92	3.83
2	1	1x10 ⁷	1.73x10 ⁷	2mL	26	95.7	99.5	57.9	20.9	0.98	1.39
3	1	1x10 ⁷	1.88x10 ⁷	2mL	27	93.1	99.1	52.7	7.83	0.98	1.20
4	2	2.5 x10 ⁷	7.26x10 ⁷	5ml	35	94.4	99.1	34.6	2.30	0.51	5.94
5	2	2.5 x10 ⁷	7.10x10 ⁷	5ml	17	93.5	99.5	35.2	15.0	1.08	4.11
6	2	2.5 x10 ⁷	2.53x10 ⁷	5ml	24	96.5	99.5	98.6	3.16	0.96	8.75

Extended Data Table 2 | Tumor measurements using mRANO criteria

Patient	SPD of baseline target lesions (cm ²)	D +1 SPD (cm ²)	D + 1 percent change in SPD*	D +28 SPD (cm ²)	D +28 percent change in SPD*	2-month SPD (cm ²)	2-month percent change in SPD*	3-month SPD (cm ²)	3-month percent change in SPD*	4-month SPD (cm ²)	4-month percent change in SPD*
1	14.40	14.39	-0.07	21.98 †	+52.64	N/A ‡	N/A ‡	--	--	--	--
2	36.23	31.11	-14.13	44.55	+22.96	23.6	-34.86	--	--	--	--
3	7.02	4.32 ¶	-38.46	N/A	N/A	5.50	-21.65	5.74	-18.23	6.37	-9.26
4	1.21	0.8	-33.88	0.7	-42.15	0.88	-27.27	0.80	-33.88	--	--
5	20.77	12.57	-39.48	19.02	-8.43	--	--	--	--	--	--
6	12.70	10.92	-14.02	10.35	-18.5	--	--	--	--	--	--

SPD = sum of products of perpendicular diameters

* compared to baseline SPD

† scan was performed on day +33 as an unscheduled assessment (out of protocol-defined window for day +28 scan)

‡ Patient had surgical resection of increasing enhancing disease between day +28 and 2-month MRI scans

¶ scan was performed on day +2, within protocol-defined window for day +1 scan

patient missed day +28 scan due to being in an acute rehab facility

Corresponding author(s): Donald O'Rourke, MDLast updated by author(s): Feb 8, 2024

Reporting Summary

Nature Portfolio wishes to improve the reproducibility of the work that we publish. This form provides structure for consistency and transparency in reporting. For further information on Nature Portfolio policies, see our [Editorial Policies](#) and the [Editorial Policy Checklist](#).

Statistics

For all statistical analyses, confirm that the following items are present in the figure legend, table legend, main text, or Methods section.

n/a | Confirmed

- The exact sample size (n) for each experimental group/condition, given as a discrete number and unit of measurement
- A statement on whether measurements were taken from distinct samples or whether the same sample was measured repeatedly
- The statistical test(s) used AND whether they are one- or two-sided
Only common tests should be described solely by name; describe more complex techniques in the Methods section.
- A description of all covariates tested
- A description of any assumptions or corrections, such as tests of normality and adjustment for multiple comparisons
- A full description of the statistical parameters including central tendency (e.g. means) or other basic estimates (e.g. regression coefficient) AND variation (e.g. standard deviation) or associated estimates of uncertainty (e.g. confidence intervals)
- For null hypothesis testing, the test statistic (e.g. F , t , r) with confidence intervals, effect sizes, degrees of freedom and P value noted
Give P values as exact values whenever suitable.
- For Bayesian analysis, information on the choice of priors and Markov chain Monte Carlo settings
- For hierarchical and complex designs, identification of the appropriate level for tests and full reporting of outcomes
- Estimates of effect sizes (e.g. Cohen's d , Pearson's r), indicating how they were calculated

Our web collection on [statistics for biologists](#) contains articles on many of the points above.

Software and code

Policy information about [availability of computer code](#)

Data collection

Data analysis

For manuscripts utilizing custom algorithms or software that are central to the research but not yet described in published literature, software must be made available to editors and reviewers. We strongly encourage code deposition in a community repository (e.g. GitHub). See the Nature Portfolio [guidelines for submitting code & software](#) for further information.

Data

Policy information about [availability of data](#)

All manuscripts must include a [data availability statement](#). This statement should provide the following information, where applicable:

- Accession codes, unique identifiers, or web links for publicly available datasets
- A description of any restrictions on data availability
- For clinical datasets or third party data, please ensure that the statement adheres to our [policy](#)

Research involving human participants, their data, or biological material

Policy information about studies with [human participants or human data](#). See also policy information about [sex, gender \(identity/presentation\), and sexual orientation](#) and [race, ethnicity and racism](#).

Reporting on sex and gender	Sex assigned at birth and self-identified gender were collected as baseline characteristics of each participant. No sex-specific analyses were performed given the overall low sample size and interim nature of the report.
Reporting on race, ethnicity, or other socially relevant groupings	Race and ethnicity were self-reported by the study participants. Categories participants could choose from included: Race: Caucasian, Black or African American, Asian, American Indian or Alaska Native, or Native Hawaiian or other Pacific Islander Ethnicity: Hispanic vs. Non-Hispanic
Population characteristics	Median age 63 (IQR, 59-76) Sex: 2 female, 5 male Race/ethnicity: all participants were white/non-hispanic Diagnosis and prior treatments: all 6 participants had diagnosis of recurrent glioblastoma, IDH-wild type and EGFR amplified. All previous therapies for each participant are provided in Table 1 in the main manuscript.
Recruitment	Potential study candidates were recruited from the neuro-oncology clinical practice at the Hospital of the University of Pennsylvania. Patients with recurrent glioblastoma and who met the study's inclusion/exclusion criteria (as outlined in the study protocol) were approached to sign informed consent for the study. Given the small sample size and phase single-arm nature of the study, it is possible that patients who elected to enroll on this trial may have better overall health, performance status, and psychosocial support relative to the general population of patients diagnosed with glioblastoma. This could result in selection bias leading to better outcomes than what may be observed in a real-world population treated with this product.
Ethics oversight	This study was approved by University of Pennsylvania Institutional Review Board

Note that full information on the approval of the study protocol must also be provided in the manuscript.

Field-specific reporting

Please select the one below that is the best fit for your research. If you are not sure, read the appropriate sections before making your selection.

Life sciences Behavioural & social sciences Ecological, evolutionary & environmental sciences

For a reference copy of the document with all sections, see nature.com/documents/nr-reporting-summary-flat.pdf

Life sciences study design

All studies must disclose on these points even when the disclosure is negative.

Sample size	The sample size for this phase 1 safety/dose-finding study was based on a traditional 3+3 design with three predefined dose levels. Given that there are 3 predefined dose levels with up to 6 patients treated at each dose level in accordance with the traditional 3+3 design, the total sample size for the trial is up to 18 patients. Such a sample size will be adequate to determine which of the 3 dose levels is the maximum tolerated dose of CART-EGFR-IL13ra2 cells.
Data exclusions	No data were excluded from the analyses.
Replication	Quantitative PCR was performed in triplicate. Cytokine expression was performed in duplicates. Immunofluorescence staining was performed in duplicates. All replication attempts were successful.
Randomization	This is a single-arm study.
Blinding	This is a single-arm study.

Reporting for specific materials, systems and methods

We require information from authors about some types of materials, experimental systems and methods used in many studies. Here, indicate whether each material, system or method listed is relevant to your study. If you are not sure if a list item applies to your research, read the appropriate section before selecting a response.

Materials & experimental systems

Methods

n/a	Involved in the study
<input type="checkbox"/>	<input checked="" type="checkbox"/> Antibodies
<input checked="" type="checkbox"/>	<input type="checkbox"/> Eukaryotic cell lines
<input checked="" type="checkbox"/>	<input type="checkbox"/> Palaeontology and archaeology
<input checked="" type="checkbox"/>	<input type="checkbox"/> Animals and other organisms
<input type="checkbox"/>	<input checked="" type="checkbox"/> Clinical data
<input checked="" type="checkbox"/>	<input type="checkbox"/> Dual use research of concern
<input checked="" type="checkbox"/>	<input type="checkbox"/> Plants

n/a	Involved in the study
<input checked="" type="checkbox"/>	<input type="checkbox"/> ChIP-seq
<input checked="" type="checkbox"/>	<input type="checkbox"/> Flow cytometry
<input type="checkbox"/>	<input checked="" type="checkbox"/> MRI-based neuroimaging

Antibodies

Antibodies used

- hIL13R α 2 for IF: R&D Systems, Catalog AF146, Lot CZT1123031, 1:50 dilution
- Anti-EGFRVIII, Absolute Antibody, Catalog AB03036-23.0, clone 806, Lot T2243A04, 1:50 dilution
- EGFRVIII peptide, Acro Biosystems, Catalog EGR-H82E0-25ug, BV3742-20CPF1-1C4, 1:50 dilution
- IL13R α 2 protein FC chimera, R&D Systems, Catalog 7147-IR-100, Lot DARK0722051, 1:50 dilution
- Anti-CD3, BioLegend, Catalog 317322, Clone OKT3
- Anti-CD4, BD Biosciences, Catalog 340133, Clone SK3
- Anti-CD8, BD Biosciences, Catalog 555634, Clone HIT8alpha
- Anti-CD45, BD Biosciences, Catalog 340943, Clone 2D1
- Biotin-GAM, Jackson ImmunoResearch, Catalog 155-065-072, F(ab')₂
- Streptavidin, BD Biosciences, Catalog 554061
- hIL13R α 2 for FCM, Sino Biological, Catalog 10350-H08H-B
- His-TAG, R&D Systems, Catalog IC050A

Validation

All antibodies were commercially available and validated by the manufacturers with details available on the manufactures' websites and/or referenced as follows:

https://www.rndsystems.com/products/human-il-13-r-alpha2-antibody_af146#product-citations

<https://pubmed.ncbi.nlm.nih.gov/11454674/>

<https://www.acrobiosystems.com/P2160-Biotinylated-Human-EGFRVIII-Protein-HisAvitag%E2%84%A2-%28MALS-verified%29.html>

https://www.rndsystems.com/products/recombinant-human-il-13-r-alpha-2-fc-chimera-cho-cf_7147-ir#product-citations

Clinical data

Policy information about [clinical studies](#)

All manuscripts should comply with the ICMJE [guidelines for publication of clinical research](#) and a completed [CONSORT checklist](#) must be included with all submissions.

Clinical trial registration

NCT05168423

Study protocol

The full study protocol is provided as an attachment.

Data collection

Data was collected at the University of Pennsylvania (Philadelphia, PA) from June, 2023 through February, 2024.

Outcomes

Primary endpoints:

- Occurrence of dose-limiting toxicities (DLTs) and determination of Maximum Tolerated Dose (MTD)
- Type, frequency, severity, and attribution of AEs/SAEs

Secondary endpoints:

- Proportion of subjects who enroll on this study who received study treatment.
- Frequency of manufacturing failures; ability to meet targeted dose and cell product volume restrictions.
- Progression-free Survival (PFS) as per modified RANO criteria
- Objective Response Rate (ORR) as per modified RANO criteria (in subjects with measurable disease at the time of study treatment)
- Duration of response (DOR) as per modified RANO criteria (in subjects with measurable disease at the time of study treatment)
- Overall Survival (OS)

Plants

Seed stocks	Report on the source of all seed stocks or other plant material used. If applicable, state the seed stock centre and catalogue number. If plant specimens were collected from the field, describe the collection location, date and sampling procedures.
Novel plant genotypes	Describe the methods by which all novel plant genotypes were produced. This includes those generated by transgenic approaches, gene editing, chemical/radiation-based mutagenesis and hybridization. For transgenic lines, describe the transformation method, the number of independent lines analyzed and the generation upon which experiments were performed. For gene-edited lines, describe the editor used, the endogenous sequence targeted for editing, the targeting guide RNA sequence (if applicable) and how the editor was applied.
Authentication	Describe any authentication procedures for each seed stock used or novel genotype generated. Describe any experiments used to assess the effect of a mutation and, where applicable, how potential secondary effects (e.g. second site T-DNA insertions, mosaicism, off-target gene editing) were examined.

Magnetic resonance imaging

Experimental design

Design type	MRI in this study was used for tumor response assessment and obtained at prespecified imaging timepoints per the study's protocol (attached)
Design specifications	MRI in this study was used for tumor response assessment and obtained at prespecified imaging timepoints per the study's protocol (attached)
Behavioral performance measures	N/A - there are no functional MRI or behavioral performance measured used in this study

Acquisition

Imaging type(s)	structural, diffusion, perfusion
Field strength	3T
Sequence & imaging parameters	Imaging protocol included axial T1-weighted 3D MPRAGE before and after contrast, post-contrast axial FLAIR, dynamic contrast-enhanced (DCE) perfusion, and dynamic susceptibility contrast (DSC) perfusion.
Area of acquisition	Whole brain scan
Diffusion MRI	<input type="checkbox"/> Used <input checked="" type="checkbox"/> Not used

Preprocessing

Preprocessing software	N/A - no preprocessing was used for the clinical MRIs obtained in this study
Normalization	N/A - no preprocessing was used for the clinical MRIs obtained in this study
Normalization template	N/A - no preprocessing was used for the clinical MRIs obtained in this study
Noise and artifact removal	N/A - no preprocessing was used for the clinical MRIs obtained in this study
Volume censoring	N/A - no preprocessing was used for the clinical MRIs obtained in this study

Statistical modeling & inference

Model type and settings	N/A - no statistical modeling or inference was used for the clinical MRI obtained in this study
Effect(s) tested	N/A - no statistical modeling or inference was used for the clinical MRI obtained in this study
Specify type of analysis:	<input checked="" type="checkbox"/> Whole brain <input type="checkbox"/> ROI-based <input type="checkbox"/> Both
Statistic type for inference	N/A - no statistical modeling or inference was used for the clinical MRI obtained in this study
(See Eklund et al. 2016)	
Correction	N/A - no statistical modeling or inference was used for the clinical MRI obtained in this study

Models & analysis

- | | |
|-------------------------------------|---|
| n/a | Involvement in the study |
| <input checked="" type="checkbox"/> | <input type="checkbox"/> Functional and/or effective connectivity |
| <input checked="" type="checkbox"/> | <input type="checkbox"/> Graph analysis |
| <input checked="" type="checkbox"/> | <input type="checkbox"/> Multivariate modeling or predictive analysis |